DEUTSCHES ELEKTRONEN-SYNCHROTRON DESY

SEARCH FOR SCALAR ELECTRONS AND PHOTINOS IN ELECTRON-POSITRON ANNIHILATIONS

by

E. Ros

Universidad Autonoma de Madrid

NOTKESTRASSE 85 · 2 HAMBURG 52

To be sure that your preprints are promptly included in the
HIGH ENERGY PHYSICS INDEX ,
send them to the following address (if possible by air mail) :

DESY
Bibliothek
Notkestrasse 85
2 Hamburg 52
Germany

SEARCH FOR SCALAR ELECTRONS AND PHOTINOS
IN ELECTRON-POSITRON ANNIHILATIONS

E. Ros

Universidad Autónoma de Madrid

ABSTRACT

We review present experimental work on
the search for scalar electrons and photinos
in electron-positron annihilations with PETRA
and PEP detectors. The absence of any signal
for these supersymmetric particles is used to
set lower limits on their masses.

CONTENTS

1-INTRODUCTION

The theories of supersymmetry [1] predict the existence of a bosonic partner for each known fermion and viceversa. This partner has the same quantum numbers except, of course, the spin. Since no such partners have been found up to now, supersymmetry must be a broken symmetry of nature.

In table I we list the known particles with their supersymmetric partners in the so-called 'minimal scheme' where a minimal number of new particles has to be introduced; we note that an additional Higgs doublet is required and that, depending on the breaking model, at least one new particle appears : for global supersymmetry, the goldstino, which is a spin-1/2 Goldstone fermion, and for local supersymmetry including gravitation, the gravitino, which is the spin-3/2 fermionic partner of the graviton.

Coupling constants and interactions between all these particles are fixed, but masses are extremely model dependent, leading to the introduction of a considerable number of free parameters. We shall limit ourselves, for the sake of simplicity, to the searches for scalar electrons $\tilde{e}$ and photinos $\tilde{\gamma}$, which have been performed by a larger number of experiments and in a more systematic way. As we shall see, even in this simple scenario of only two supersymmetric particles, a lot of possibilities are still to be considered for experiment.

We have used results obtained in electron-postitron annihilations with the CELLO, JADE, MARK J and TASSO detectors at the PETRA storage ring (with beam energy up to 23.3 Gev) and with the MAC and MARK II detectors at PEP storage ring (the beam energy being 14.5 Gev).

particle	spin	name	s-particle	spin	name
q_L, q_R	1/2	quarks	$\tilde{q}_L, \tilde{q}_R$	0	s-quarks
l_L, l_R	1/2	leptons	$\tilde{l}_L, \tilde{l}_R$	0	s-leptons
ν_L	1/2	neutrinos	$\tilde{\nu}_L$	0	s-neutrinos
g	1	gluon	$\tilde{g}$	1/2	gluino
W	1	weak	$\tilde{W}$	1/2	Wino
Z	1	bosons	$\tilde{Z}$	1/2	Zino
γ	1	photon	$\tilde{\gamma}$	1/2	photino
H_1^0, H_1^+	0	Higgs	$\tilde{H}_1^0, \tilde{H}_1^+$	1/2	Higgsinos
H_2^-, H_2^0	0	bosons	$\tilde{H}_2^-, \tilde{H}_2^0$	1/2	

Table I

2-PRODUCTION OF PHOTINOS AND SCALAR ELECTRONS IN e^+e^- ANNIHILATIONS

Four types of production processes for scalar electrons and photinos have been proposed in e^+e^- annihilations. These processes with the corresponding references are :

$$e^+e^- \rightarrow \tilde{e}\tilde{e} \qquad [2] \quad [3]$$
$$e^+e^- \rightarrow \tilde{\gamma}\tilde{\gamma} \qquad [4] \quad [5]$$
$$\gamma e \rightarrow \tilde{\gamma}\tilde{e} \qquad [6] \quad [7]$$
$$\gamma\gamma \rightarrow \tilde{e}\tilde{e} \qquad [3]$$

For the last two processes the radiating electron goes into the beam line and remains undetected; the photons are of course virtual and are usually treated in the Weiszsäcker-Williams approximation [21]. In table II we quote for all these processes the Feynman diagrams, angular distributions as a function of the t invariant, also expressed as function of $y = \cos\theta$, θ being the center-of-mass scattering angle, and finally total cross-sections. We have assumed everywhere that $m_e = 0$ and that $\tilde{e}_R$ and $\tilde{e}_L$ have the same mass, which is the most favourable situation for experiment. The most unfavourable situation arises when the masses are different and one of them goes to infinity; the cross-section is then normally obtained from the degenerated case dividing by a factor 2. We also used the following notations :

$$\Sigma = m_{\tilde{e}}^2 + m_{\tilde{\gamma}}^2 \qquad \Delta = m_{\tilde{e}}^2 - m_{\tilde{\gamma}}^2 \qquad \sigma_{pt} = \frac{4}{3}\pi\frac{\alpha^2}{s}$$

Derivations of the cross-section formulas for the above mentioned processes can de found in the appendix. Here we only make the following remarks :

For the scalar electron pair production, beside the usual photon exchange diagram, common to all other processes where a scalar particle like $\tilde{\mu}$ or $\tilde{\tau}$ is produced, there exists a t channel diagram which depends on the photino mass and which can create important modifications in the angular distribution, specially if the photino mass is low. The total cross-section includes not only $\tilde{e}_R\tilde{e}_R$ and $\tilde{e}_L\tilde{e}_L$ production, but also $\tilde{e}_R\tilde{e}_L$ production ,which gives a term proportional to $m_{\tilde{\gamma}}^2$; if one of the two scalar partners of the electron acquires an infinite mass, this term will therefore vanish even for $m_{\tilde{\gamma}} \neq 0$.

For the photino pair production, there are two exchanged diagrams, as the photino is identical to its antiparticle (and mathematically described by a Majorana spinor). The cross-section is sensitive to the scalar electron mass via the propagator.

The photoproduction of scalar electron and photino is interesting since more energy is available for the production of one of the two particles, in the case where the other is light; the quoted cross-section is valid for an $e^+\gamma$ or $e^-\gamma$ collision. In e^+e^- interactions both processes arise and so an additional factor 2 is to be considered if no charge requirement is imposed.

The production of a scalar pair in photon-photon collisions is included here only for completeness, since no experimental search using this process has been performed up to now, the reason being that the mass region covered is the same than in the first process which already provides a very clear signal.

3-FINAL STATES

In fig.Ia we show the regions in the $m_{\tilde{e}} - m_{\tilde{\gamma}}$ plot which can be kinematically accessed for a given beam energy E_b; for the processes $e^+e^- \rightarrow \tilde{e}\tilde{e}$ and $\tilde{\gamma}\tilde{\gamma}$ these regions are $m_{\tilde{e}} < 2E_b$ and $m_{\tilde{\gamma}} < 2E_b$ respectively (the limit in the $\tilde{e}\tilde{e}$ case is almost independent of the photino mass) while for $e^+e^- \rightarrow \tilde{\gamma}\tilde{e}(e)$ the limit is $m_{\tilde{e}} + m_{\tilde{\gamma}} < 2E_b$.

From an experimental point of view it is necessary to know the final states, that is how $\tilde{e}$ and $\tilde{\gamma}$ decay. We have then to consider several possibilities :

If $m_{\tilde{e}} > m_{\tilde{\gamma}}$, $\tilde{e}$ will decay into $\tilde{e}\tilde{\gamma}$ with a decay amplitude :

$$\Gamma_{\tilde{e}} = \frac{\alpha}{2}m_{\tilde{e}}\left(1 - \frac{m_{\tilde{\gamma}}^2}{m_{\tilde{e}}^2}\right)^3$$

4

the lifetime will be $4.5 \ 10^{-24}$ sec for $m_{\tilde{e}} = 40$ Gev and $m_{\tilde{\gamma}} = 0$. The stability of the photino will depend on the existence of a lighter particle, like the goldstino G, as proposed in reference [9]; if the goldstino is lighter, the photino will decay into γG with a decay amplitude :

$$\Gamma_{\tilde{\gamma}} = \frac{m_{\tilde{\gamma}}^5}{8\pi d^2}$$

where the d parameter gives the scale of supersymmetry breaking and one can take $d = (100 \ \text{Gev})^2$ for example purposes; the lifetime of the photino is then $\tau_{\tilde{\gamma}} = 1.65 \ 10^{-15} sec/m_{\tilde{\gamma}}^5 (Gev)$. We note that the decay path of a 100 Mev photino at 20 Gev is 10 meters escaping detection for normal detectors.

If $m_{\tilde{e}} < m_{\tilde{\gamma}}$, $\tilde{e}$ is probably a stable particle (it is certainly in the absence of any other supersymmetric particle like $\tilde{\nu}$) with properties concerning detection very similar to those of a muon. On the other side the photino will decay into $\tilde{e}\gamma$ with decay amplitude:

$$\Gamma_{\tilde{\gamma}} = \alpha m_{\tilde{\gamma}} \left(1 - \frac{m_{\tilde{e}}^2}{m_{\tilde{\gamma}}^2}\right)^2$$

in competition with the above mentioned mode γG; in figure Ib we show these dominant modes.

In fig.Ic and Id all the possible final states for the processes $e^+e^- \rightarrow \tilde{e}\tilde{e}, \tilde{\gamma}\tilde{\gamma}$ and $\tilde{e}\tilde{\gamma}(e)$ are presented for both cases $m_{\tilde{\gamma}} < m_G$ and $m_{\tilde{\gamma}} > m_G$. Not all these cases have been experimentally analysed. In fact the only case which has been fully investigated is $m_G > m_{\tilde{e}} > m_{\tilde{\gamma}}$, that is the stable and undetectable photino case. The signatures for the different processes are then:
$e^+e^- \rightarrow \tilde{e}\tilde{e}$: pair of electrons with missing energy as proposed in reference [2]
$e^+e^- \rightarrow \tilde{\gamma}\tilde{e}(e)$: a single electron as proposed in reference[6]
$e^+e^- \rightarrow \tilde{\gamma}\tilde{\gamma}$: nothing except if one electron radiates a photon. The signature is then a single photon as proposed in reference [4]

Other situations which have drawn experimental attention and that we shall therefore consider are :
$e^+e^- \rightarrow \tilde{e}\tilde{e}$: pair of stable $\tilde{e}$, the signature being a $\mu\mu$-like back-to-back event
$e^+e^- \rightarrow \tilde{\gamma}\tilde{\gamma}$: pair of unstable $\tilde{\gamma}$ decaying into a photon and an invisible particle, the signature being a pair of photons with missing energy.

Next we give values for the cross-sections in the case of a light and stable photino, the most popular situation as we just said.

4-THE LIGHT PHOTINO CASE

Most of the theoretical and experimental effort has been devoted to the case of a light and stable photino with a heavy scalar electron decaying into $e\tilde{\gamma}$. Although a strictly null mass for the photino is not expected since it will acquire one, at least by radiative corrections, we will take $m_{\tilde{\gamma}} = 0$ since this approximation leads to important simplifications in the cross-section formulas.

For the process $e^+e^- \rightarrow \tilde{e}\tilde{e}$, we have :

$$\sigma_{\tilde{e}\tilde{e}} = \frac{3}{8}\sigma_{pt}\{-\beta_{\tilde{e}}(10 + \frac{2}{3}\beta_{\tilde{e}}^2) + [4 + (1 + \beta_{\tilde{e}}^2)^2]\ln\frac{1+\beta_{\tilde{e}}}{1-\beta_{\tilde{e}}}\}$$

If we are close to the production threshold, $\beta_{\tilde{e}} \rightarrow 0$ and we have $\sigma_{\tilde{e}\tilde{e}} \approx 5/2\beta_{\tilde{e}}^3\sigma_{pt}$ exhibiting the typical $\beta_{\tilde{e}}^3$ behaviour of scalar particles. On the contrary, if $\beta_{\tilde{e}} \rightarrow 1 (m_{\tilde{e}} \rightarrow 0$ or $s \rightarrow \infty)$, one has a logarithmic rise of the cross-section : $\sigma_{\tilde{e}\tilde{e}} = 3\sigma_{pt}(\ln s/m_{\tilde{e}}^2 - 4/3)$.

For the process $\gamma e \rightarrow \tilde{\gamma}\tilde{e}$, one has :

$$\sigma_{\tilde{\gamma}\tilde{e}} = \frac{3}{4}\sigma_{pt}[(1 - \frac{m_{\tilde{e}}^2}{s})(1 + 7\frac{m_{\tilde{e}}^2}{s}) + 4\frac{m_{\tilde{e}}^2}{s}(1 + \frac{m_{\tilde{e}}^2}{s})\ln\frac{m_{\tilde{e}}^2}{s}]$$

In this case it is possible to integrate analytically the cross-section over the quasi-real photon spectrum; so in e^+e^- interactions and summing over the two charged states:

$$\sigma_{\tilde{\gamma}\tilde{e}(e)} = 2\int_\mu^1 dx f_\gamma(x)\sigma_{\tilde{\gamma}\tilde{e}}(xs) \quad \text{with} \quad f_\gamma(x) = \frac{\alpha}{2\pi}\log\frac{s}{4m_e^2}[\frac{1 + (1-x)^2}{x}] \quad \text{and} \quad \mu = \frac{m_{\tilde{e}}^2}{s}$$

$$= \frac{\alpha}{6\pi}\sigma_{pt}\ln\frac{s}{4m_e^2}[\frac{2}{\mu} + 18 - 54\mu + 34\mu^2 + 3(3 - 3\mu - 4\mu^2)\ln\mu - 9\mu\ln^2\mu]$$

5

Of course, the above cross-sections are total cross-sections and the experimentally visible part will only be a fraction of it, depending on the detector acceptance. We note however that for values of $m_{\tilde{e}}$ close to the beam energy one will obtain isotropic particles in the final state, independent of the primary particle distributions. These final states, as we said before, are pairs of electrons in the $\tilde{e}\tilde{e}$ case and a single electron in the $\tilde{\gamma}\tilde{e}$ case. The energy of these electrons will approach the value $m_{\tilde{e}}/2$ as $m_{\tilde{e}}$ increases. In the electron pair case it is usual to impose an additional acoplanarity cut in order to reduce QED background. As an example, for an acceptance of $|y| < 0.8$ and an acoplanarity cut of 40 degrees, the efficiency will be $\epsilon = (0.8)^2 0.78 = 50\%$ for electron pairs and $\epsilon = 80\%$ for isolated electrons. In practice a lot of additional cuts are used in selecting the data, but they are extremely detector dependent.

For the process $e^+ e^- \rightarrow \tilde{\gamma}\tilde{\gamma}$, one has :

$$\sigma_{\tilde{\gamma}\tilde{\gamma}} = \frac{3}{2}\sigma_{pt}[1 + \frac{1}{1+\eta} - \frac{2}{\eta}\ln(1+\eta)] \qquad \text{where} \quad \eta = \frac{s}{m_{\tilde{e}}^2}$$

We can also write :

$$\sigma_{\tilde{\gamma}\tilde{\gamma}} = \sigma_{loc}G(\eta) \qquad \text{with} \quad G(\eta) = \frac{3}{\eta^2}[1 + \frac{1}{1+\eta} - \frac{2}{\eta}\ln(1+\eta)] \quad \text{and} \quad \sigma_{loc} = \frac{2}{3}\frac{\pi\alpha^2}{m_{\tilde{e}}^4}s$$

σ_{loc} is the 'local' approximation cross-section, for $m_{\tilde{e}} \gg s$, in which case $G(\eta) \rightarrow 1$. As we noted before, nothing is seen in the final state unless a photon is radiated, as suggested in references [4] and [5]. The complete calculation for this process can be found in reference [8]; an approximated value which becomes exact in in the local limit can be worked out using the Bonneau-Martin formula for initial state radiation [22]. Then the single photon cross-section becomes:

$$\frac{d\sigma_\gamma}{dx dy} = \frac{2\alpha}{\pi}\frac{[(1-\frac{x}{2})^2 + \frac{1}{4}x^2 y^2]}{x(1-y^2)}\sigma_{\tilde{\gamma}\tilde{\gamma}}[s(1-x)]$$

Integration for $|y| < y_m$ leads to :

$$\frac{d\sigma_\gamma}{dx} = \frac{2\alpha}{\pi}\left[(\frac{1}{x} - 1 + \frac{x}{2})\log\frac{1+y_m}{1-y_m} - y_m\frac{x}{2}\right]\sigma_{\tilde{\gamma}\tilde{\gamma}}[s(1-x)]$$

which can be integrated numerically for $x > x_m$.

In figures IIa and IIb we give the cross-sections for all these processes, first for a fixed scalar electron mass of 40 Gev as a function of the beam energy , and then for a fixed beam energy value of 20 Gev, as a function of the scalar electron mass. In figure IIc we compare the cross-sections for the processes $e^+ e^- \rightarrow \tilde{\gamma}\tilde{\gamma}\gamma$ and $\nu\bar{\nu}\gamma$ which is the most dangerous background; the cross-section for this last process is [10]:

$$\frac{d\sigma_\gamma}{dx} = \frac{2\alpha}{\pi}\left[(\frac{1}{x} - 1 + \frac{x}{2})\log\frac{1+y_m}{1-y_m} - y_m\frac{x}{2}\right]\sigma_{\nu\bar{\nu}}[s(1-x)]$$

Where $\sigma_{\nu\bar{\nu}}$ is the neutrino-antineutino production cross-section :

$$\sigma_{\nu\bar{\nu}}(s) = \frac{G_F^2 s}{48}\pi\left[\frac{4s/M_Z^2 - 1}{(1 - s/M_Z^2)^2 + \Gamma_Z^2/M_Z^2} + 8\right]$$

The photon spectrum is peaked at small angles and energies, so the x_m, y_m cuts play here a very important role; we have taken typical values of $x_m = 0.2$ and $y_m = 0.8$. As we can see an optimal signal to background ratio is reached at PETRA energies. The complete set of Feynman diagrams contrbuting to the process $e^+ e^- \rightarrow \tilde{\gamma}\tilde{\gamma}\gamma$ can be found in figure IId.

5-EXPERIMENTAL LIMITS

UNSTABLE SCALAR ELECTRON PAIR PRODUCTION

If the scalar electron mass is below the beam energy, it can be pair-produced according to $e^+e^- \to \tilde{e}\tilde{e}$ and decay into $e\tilde{\gamma}$; the photino will escape detection, and the signature of the event will be a pair of electrons with missing energy.

Possible background sources for this process are (fig.IIIa) :

$$e^+e^- \to ee$$
$$\to ee(\gamma)$$
$$\to ee(ee)$$
$$\to \tau\tau \to ee(4\nu)$$
$$\to ee(\gamma\gamma)$$

Bbabha events ($e^+e^- \to ee$) can be easily rejected by an acoplanarity cut; for example, 99% of the Bhabha cross-section is inside the region $acop. < 10^o$; hard radiative Bhabhas are a serious background only if the detector has holes in calorimetry where the photon can escape (in fig.III a typical detector with holes is shown) but one can still reconstruct the missing particle direction; the two photon process $ee \to ee(ee)$ and $\tau\tau$ decays in the ee mode can also be cut away by the acoplanarity criterium; finally, double radiative Bhabhas where both photons escape detection are rather rare events.

For the high mass case ($m_{\tilde{e}} \approx E_b$) one expects 2 energetic electrons with $E \to m_{\tilde{e}}/2$ if $m_{\tilde{\gamma}}$ stays small and a rather flat distribution in angle and acoplanarity; for the low mass case ($m_{\tilde{e}} \ll E_b$) one expects a back-to-back topology where only missing energy can discriminate with Bhabha type events; in any case it is not possible to separate this signal from $\gamma\gamma$ processes and $\tau\tau$ decays in the ee mode mentioned above. This case is normally not treated in experimental analysis.

Among the various searches, we report the following :

JADE [13] has looked for electron pairs within the acceptance cuts $E > 0.25E_b$, $|y| < 0.75$, $acop > 40^o$, plus additional cuts to reject events if the missing energy points towards a hole of the detector; the integrated luminosity used is 87 pb^{-1} at energies in the region $\sqrt{s} = 32 - 46.8$ Gev.

CELLO [11] analysis requires $E > 0.10E_b$, $|y| < 0.85$, $35^o < acop < 170^o$, using a luminosity of 10 pb^{-1} at energies $\sqrt{s} = 44 - 46.8$ Gev with a complete calorimetric coverage down to 3°, and additional 8 pb^{-1} with holes in the region between 22° and 30°.

The obtained limits are shown in figure IVa; the main limitation is beam energy; the low mass case is not covered in these analysis for the reasons mentioned before; it is also interesting to note the enhancement of the cross-section as $m_{\tilde{\gamma}}$ increases due to the production of $\tilde{e}_R\tilde{e}_L$, in addition to $\tilde{e}_R\tilde{e}_R$ and $\tilde{e}_L\tilde{e}_L$.

Previous analysis by CELLO and TASSO can be found in references [23] and [24].

UNSTABLE SINGLE SCALAR ELECTRON PRODUCTION

A single scalar electron can be produced in association with a photino in the process $e^+e^- \to \tilde{e}\tilde{\gamma}(e)$; this process allows to reach $m_{\tilde{e}}$ values above the beam energy provided $m_{\tilde{\gamma}}$ stays small. The signature of the event will be a single electron.

Possible backgrounds sources are (fig.IIIb) :

$$e^+e^- \to e(e\gamma)$$

where one electron escapes along the beam line and the photon goes through a hole of the detector or also along the beam line. To be protected against the first type of background, the detector must have as few holes as possible; concerning the second type, it must be possible to tag particles at small angles; a 3° tag, for example, allows a minimum p_T cut for the single electron of $x_T = p_T/E_b = 2\sin 3^o = .10$

. For an $\tilde{e}$ decay electron, one expects a rather flat distribution in angle, peaked in energy at $m_{\tilde{e}}/2$, specially if the $\tilde{e}$ mass is high. The spectrum is quite favourable since the single electron spectrum coming from QED is

7

peaked at small angles and energies; so the search is possible even with holes in the detector, provided enough statistics is available, as in the MARK II analysis.

The following searches have been made :

JADE [13] has looked for single electrons within the cuts $|y| < 0.70$, $p_T > 0.65E_b$ with a total integrated luminosity of 73 pb^{-1} in the energy region $\sqrt{s} = 32 - 38.6$ Gev.

CELLO [11] required $|y| < 0.85$, $E > .28E_b$, $p_T > .23E_b$, with a luminosity of 10 pb^{-1} mainly at an energy of $\sqrt{s} = 44$ Gev and complete calorimetric coverage until $3°$.

The results are shown in fig.IVb; in addition two former searches were done at PEP :

MARK II [17] required $|y| < 0.70$, $E > .41E_b$, plus additional cuts due to their holes in calorimetry, spetially in the region y=0.71 − 0.75, and looked preferently at electrons in the backward direction. Their final result with a luminosity of 123 pb^{-1} at a $\sqrt{s} = 29$ Gev center of mass energy is $m_{\tilde{e}} > 22.2$ Gev for $m_{\tilde{\gamma}} = 0$.

MAC [18] with a luminosity of 36.4 pb^{-1} at the same beam energy, required $|y| < 0.75$ and $E > .21E_b$ with a complete calorimetric coverage (98% of 4π); their result is $m_{\tilde{e}} > 22.4$ Gev also for $m_{\tilde{\gamma}} = 0$.

RADIATIVE STABLE PHOTINO PAIR PRODUCTION

In the case where $\tilde{\gamma}$ is stable, the signature for photino pair production can be an isolated photon. Possible background sources are (fig IIIc) :

$$e^+ e^- \rightarrow \gamma(\gamma\gamma)$$
$$\rightarrow \gamma(ee)$$
$$\rightarrow \gamma(\nu\bar{\nu})$$

in addition to cosmic background, which can be removed by time of flight counters, or looking at hits in the muon chambers, inner detector, etc... To carry on this search a complete calorimetric coverage and tagging at small angles are very important since the photon spectrum will not differ from QED background (peaked at small energies and angles) as a difference to the previous single electron analysis. Concerning the neutrino background, it cannot be separated from the photino signal, but this background is small at PETRA and PEP energies as discussed previously.

The following analysis have been made :

JADE [13], with holes in calorimetry, looked inside the region $|y| < 0.7$, $E_T > 0.6E_b$ with a total luminosity of 46 pb^{-1} in the energy range $\sqrt{s} = 32 - 46$ Gev.

CELLO [11], with complete calorimetric coverage and 10 pb^{-1} at a center of mass energy of $\sqrt{s} = 44$ Gev, required $E_T > .9E_b$ and $|y| < 0.85$.

MAC [19], with a center of mass energy of $\sqrt{s} = 29$ Gev required $|y| < 0.75$, $E_T > 0.31E_b$ for a first set of data (36 pb^{-1}) where the calorimetric coverage reached the $10°$ angle, and $E_T > 0.21E_b$ for a second set (80 pb^{-1}) with coverage until $5°$. After these cuts one event with $E_T = 0.37E_b$ survived. Additional background sources were analysed, with the following result :

$$
\begin{array}{rcll}
ee\gamma \text{(detector inefficiencies)} & < & 0.05 & events \\
\tau\tau\gamma & < & 0.05 & events \\
\mu\mu\gamma & < & 0.10 & events \\
\text{beam gas, beam halo} & < & 0.10 & events \\
\nu\bar{\nu}\gamma & = & 0.50 & events \\
\end{array}
$$

This single event was therefore treated as a background event.

The results from these analysis are shown in fig.IVc; we note that the MAC limit is a 90% CL limit, while all other limits quoted in this note are 95% CL limits.

A new experiment on single photon detection with the ASP detector [20], has started data taking in the PEP beam in october 84; this detector is essentially an hermetic lead glass calorimeter and will it make possible to reach the 60 − 65 Gev region for the scalar electron mass after collection of 100 pb^{-1}.

STABLE SCALAR ELECTRON PAIR PRODUCTION

If the scalar electron has a mass smaller than the photino one, it will probably be a stable particle; the signature for a scalar electron pair event will then be a pair of minimum ionizing particles, like a pair of muons. If $m_{\tilde{e}}$ is low it is in fact not possible to separate this signal from the muon one, but a significant enhancement in the muon pair cross-section is expected. If $m_{\tilde{e}}$ is high (close to E_b), it is possible to measure β by usual techniques (time of flight counters, dE/dx measurements).

The only analysis on this kind of signal is for the moment the JADE analysis. For the high mass case JADE [13] has looked for 2 acoplanar non showering tracks with $E > 0.33E_b$, $|y| < 0.76$; the dE/dx measurement is reliable for β values under 0.7 which correspond to a mass $m_{\tilde{e}} > 0.7E_b$. The luminosity used is 65 pb^{-1} at a center of mass energy $\sqrt{s} = 34.5 - 46.8$ Gev. For the low mass case JADE has looked for an enhancement in the muon pair cross-section measured at $\sqrt{s} = 34.5$ Gev, which was consistent with the QED prediction within a 5% error (this excludes the region $m_{\tilde{e}} < 9$ Gev for the undegenerated case). The intermediate mass range is covered by an analysis based on TOF counters.

The final limit is shown in figure IVd; this result does not depend on the photino mass, as we already noted, due to the photon exchange diagram.

UNSTABLE PHOTINO PAIR PRODUCTION

If the photino is unstable and decays into $G\gamma$, G being a light and undetected particle like the goldstino, the signature for photino pair production will be a pair of photons with missing energy. Possible background sources are :

$$e^+ e^- \rightarrow \gamma\gamma$$
$$\rightarrow \gamma\gamma(\gamma)$$
$$\rightarrow \gamma\gamma(ee)$$

in addition to cosmic showering events, which can be removed in the way described before for the single photon analysis; $\gamma\gamma$ events are easily rejected since for example 99% of them lay inside the region $acop. < 10^o$; $\gamma\gamma$ events with hard radiation are only a problem if the detector has holes, and finally $\gamma\gamma(ee)$ events where both electrons escape detection are rather rare events.

For the high mass case $(m_{\tilde{\gamma}} \rightarrow E_b)$ one expects 2 energetic photons $(E \rightarrow m_{\tilde{\gamma}}/2)$ with rather flat distributions in angle and acoplanarity; for the low mass case $(m_{\tilde{\gamma}} \ll E_b)$ one expects a back-to-back topology where missing energy is the only criterium to distinguish from $\gamma\gamma$ QED events; the search, however, can be performed also in this second case once cosmics are removed since there is no additional background (this was not the case for the electron pairs).

The following searches have been made :

CELLO [11] has looked for photon pairs within the region $E > 0.1E_b$, $|y| < 0.85$ at a center of mass energy of $\sqrt{s} = 44 - 46$ Gev, with a luminosity of 13.5 pb^{-1} and complete calorimetric coverage. For the high mass case the cut applied is $10^o < acop < 165^o$ and for the low mass case $acop < 10^o$, $acol < 20^o$, and $E_1 + E_2 < 1.5E_b$. A previous analysis can be found in reference [25].

JADE [12] analysis requires $E > 0.25E_b$, $|y| < 0.76$ and $acop > 10^o$ plus additional cuts to avoid holes, for the high mass case. For the low mass one the cuts are $acol < 10^o$, $E_1E_2 < 0.6E_b^2$. The luminosity used is 79 pb^{-1} at center of mass energies of $\sqrt{s} = 32 - 43$ Gev.

TASSO [14] applied the cuts $|y| < 0.65$, $E > 0.1E_b$ and $E_1 + E_2 < 1.33E_b - 8acol$; if $acol < 1^0$ one of the showers must have more than 9 Gev and the other less than 16 Gev. The calorimetric coverage in Φ is only 60% and the luminosity used is 13.6 pb^{-1} at energies $\sqrt{s} = 40 - 46$ Gev.

MARK J [15] required $acol > 30^o$; other searches with this detector are listed in reference [16].

In fig.IVe we show the limits obtained with the previous searches. A value of $(100 \text{ Gev})^2$ is assumed for the d parameter entering the photino decay formula. In this case the decay path of 1 meter, which is the size of a typical calorimeter, is reached for masses under 150 Mev. The range of d-values to which present detectors are sensitive is shown in fig.IVf, as a function of $m_{\tilde{\gamma}}$; the upper bound is fixed by beam energy and the lower bound by the size of the detector; this lower bound can be improved a little bit by looking at single photons as it is done in the JADE analysis [12].
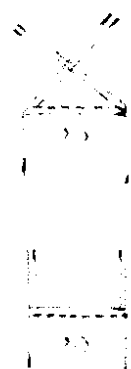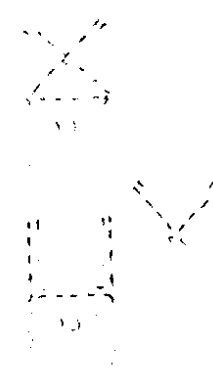
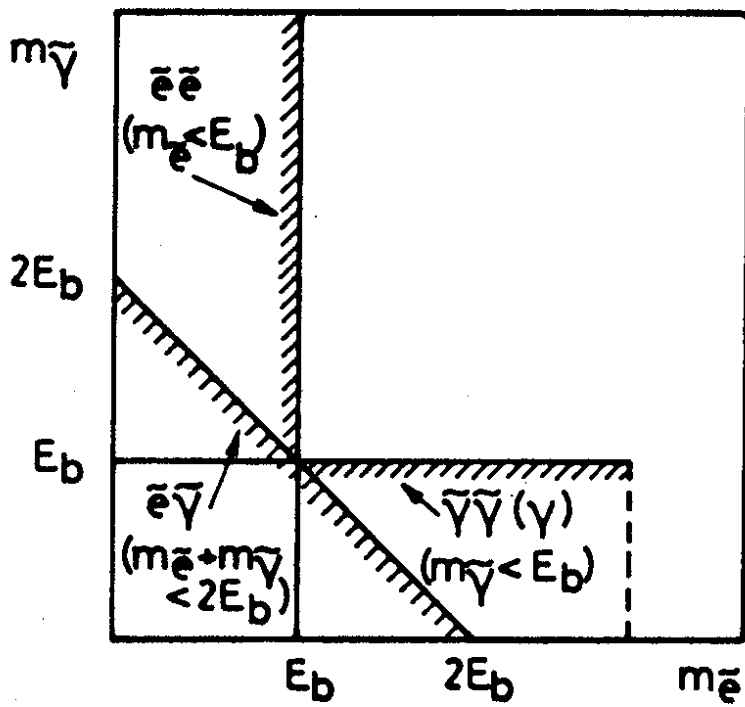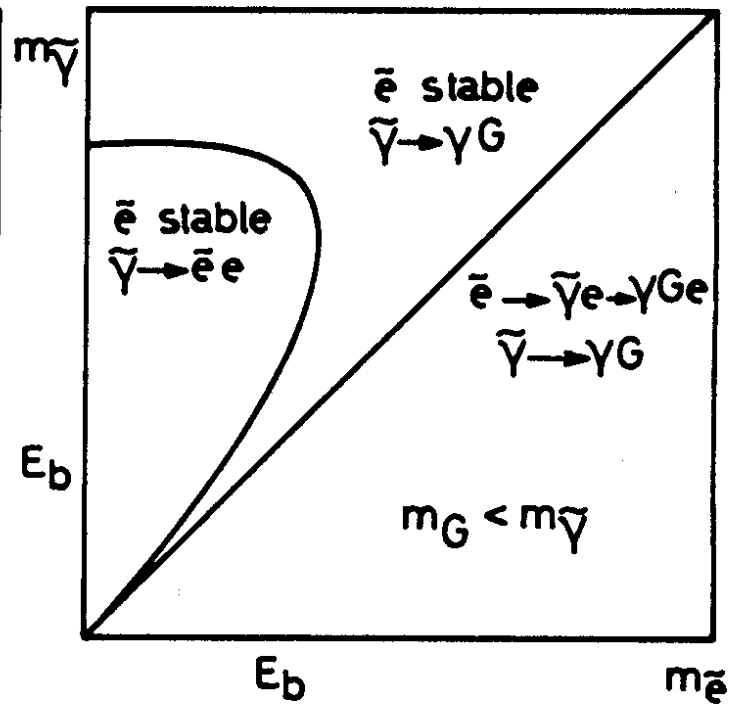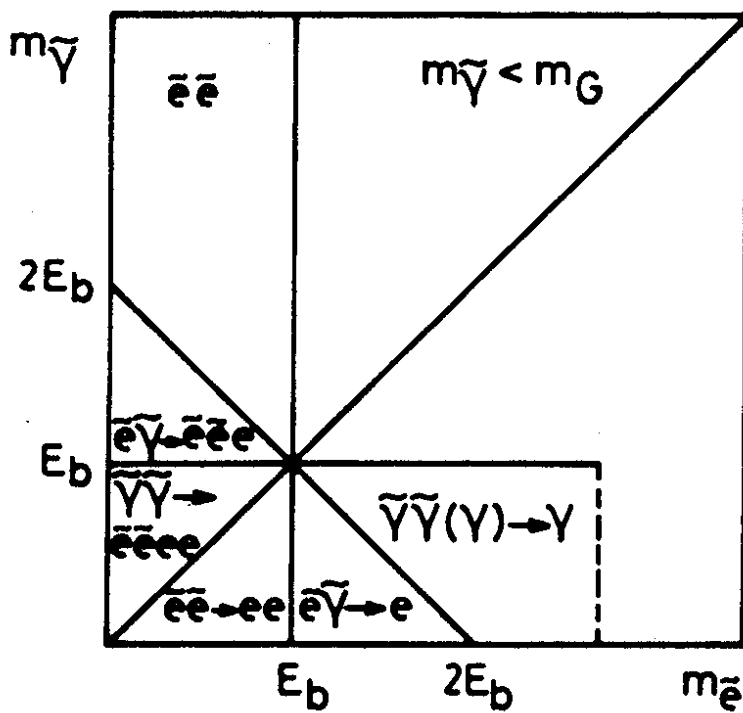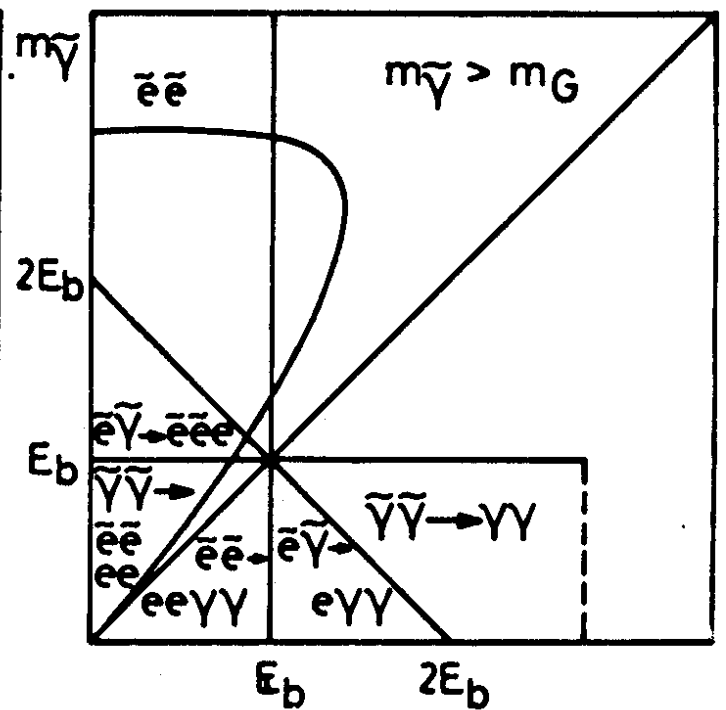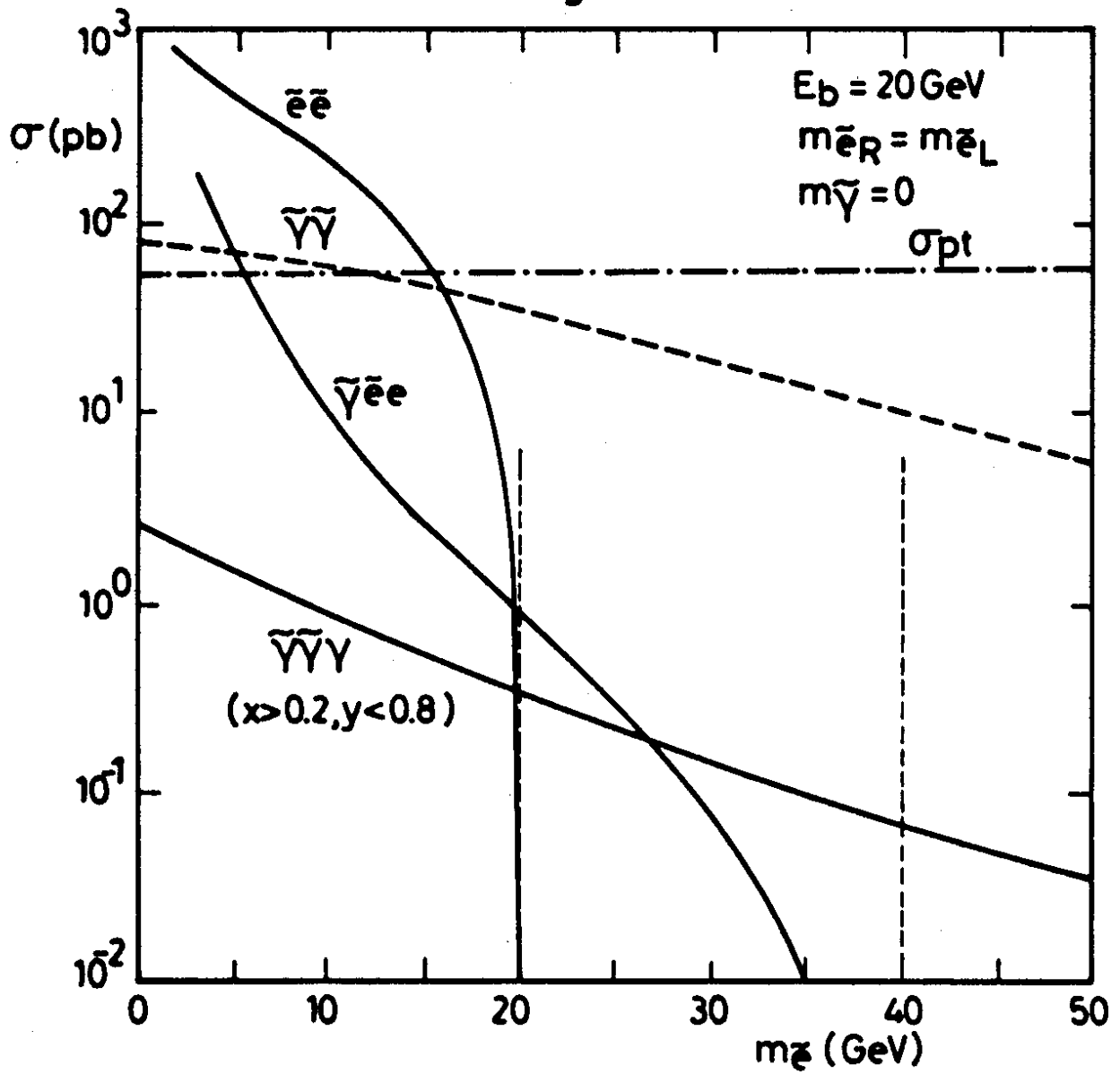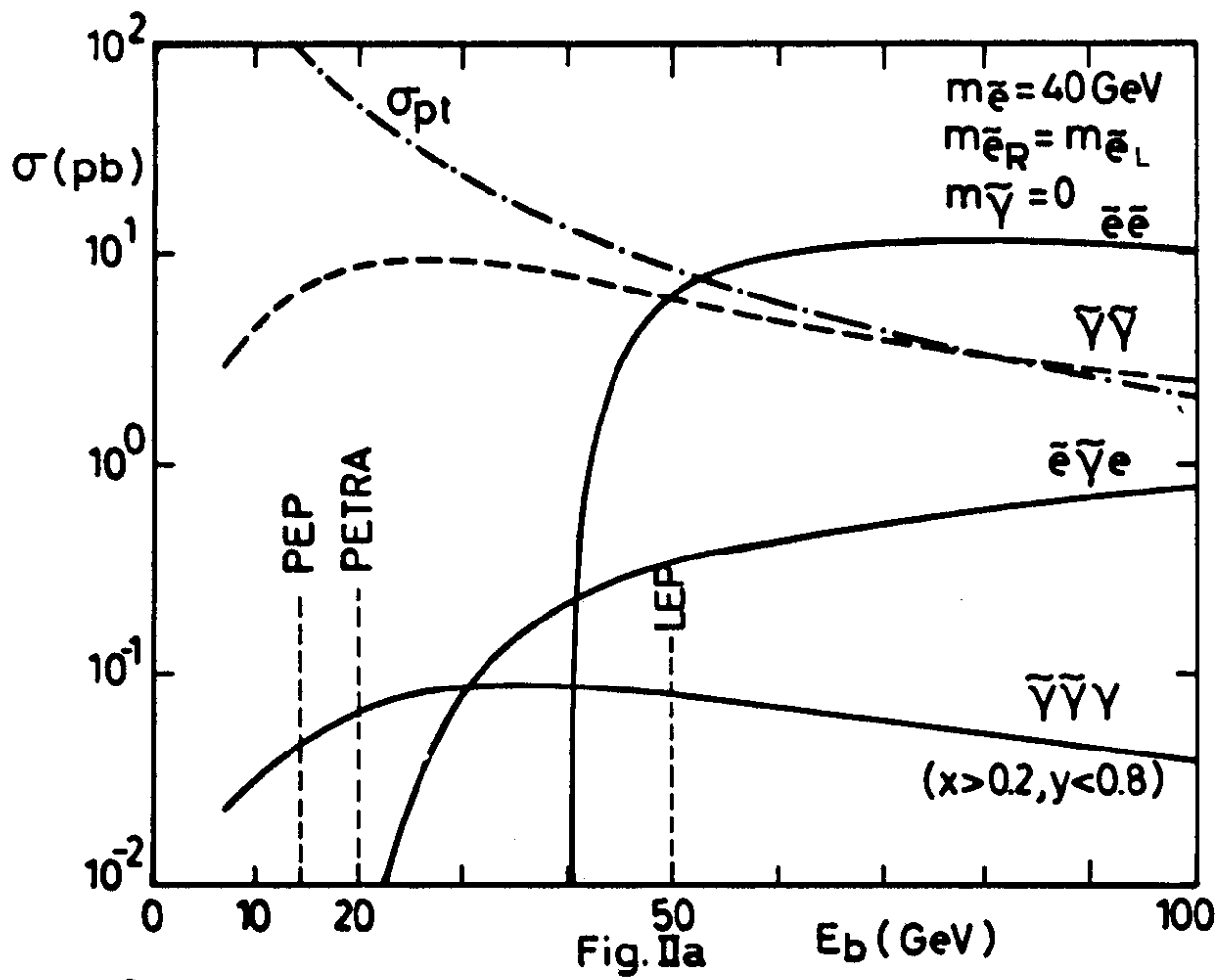| process	Feynman diagrams	angular distribution	total cross-section
$e^+e^- \to \tilde{e}\tilde{e}$		$$\frac{d\sigma}{dt} = \frac{2\pi\alpha^2}{s^2}\left\{\left[1 + \left(1+\frac{s}{t-m_{\tilde{\gamma}}^2}\right)^2\right]\left[\frac{ut-m_{\tilde{e}}^4}{s^2}\right] + \frac{sm_{\tilde{\gamma}}^2}{(t-m_{\tilde{\gamma}}^2)^2}\right\}$$ $$t = (p_{\tilde{e}} - p_e)^2 = m_{\tilde{e}}^2 - \frac{s}{2}(1-\beta_{\tilde{e}}y)$$	$$\sigma = \frac{3}{4}\sigma_{pt}\beta_{\tilde{e}}\left\{-\left(5+\frac{\beta_{\tilde{e}}^2}{3}+4\frac{m_{\tilde{\gamma}}^2}{s}\right) + \frac{8m_{\tilde{\gamma}}^2/s}{(1-2\frac{\Delta}{s})^2-\beta_{\tilde{e}}^2}\right.$$ $$\left. + \frac{1}{\beta_{\tilde{e}}}\left[1+\frac{4m_{\tilde{\gamma}}^2}{s}+(1-2\frac{\Delta}{s})^2\right]\ln\frac{\Delta-\frac{s}{2}(1+\beta_{\tilde{e}})}{\Delta-\frac{s}{2}(1-\beta_{\tilde{e}})}\right\}$$
$e^+e^- \to \tilde{\gamma}\tilde{\gamma}$		$$\frac{d\sigma}{dt} = \frac{2\pi\alpha^2}{s^2}\left[\frac{(t-m_{\tilde{\gamma}}^2)^2}{(t-m_{\tilde{e}}^2)^2} + \frac{(u-m_{\tilde{\gamma}}^2)^2}{(u-m_{\tilde{e}}^2)^2} - \frac{2m_{\tilde{\gamma}}^2 s}{(t-m_{\tilde{e}}^2)(u-m_{\tilde{e}}^2)}\right]$$ $$t = (p_{\tilde{\gamma}} - p_e)^2 = m_{\tilde{\gamma}}^2 - \frac{s}{2}(1-\beta_{\tilde{\gamma}}y)$$	$$\sigma = 3\sigma_{pt}\beta_{\tilde{\gamma}}(\Delta^2 + \frac{s}{2}m_{\tilde{e}}^2)\left[\frac{1}{\Delta^2+sm_{\tilde{e}}^2}\right.$$ $$\left. - \frac{1}{s\beta_{\tilde{\gamma}}(\Delta+\frac{s}{2})}\ln\frac{\Delta+\frac{s}{2}(1+\beta_{\tilde{\gamma}})}{\Delta+\frac{s}{2}(1-\beta_{\tilde{\gamma}})}\right]$$
$\gamma e \to \tilde{\gamma}\tilde{e}$		$$\frac{d\sigma}{dt} = \frac{2\pi\alpha^2}{s^2}\left[\frac{m_{\tilde{\gamma}}^2-u}{s} + \frac{(t-m_{\tilde{\gamma}}^2)(t+m_{\tilde{e}}^2)}{(t-m_{\tilde{e}}^2)^2}\right.$$ $$\left. - \frac{(t-m_{\tilde{e}}^2)(s-2\Delta)+2sm_{\tilde{e}}^2}{s(t-m_{\tilde{e}}^2)}\right]$$ $$t = (p_{\tilde{\gamma}} - p_e)^2 = m_{\tilde{e}}^2 - \frac{s}{2}(1+\frac{\Delta}{s})(1-\beta_{\tilde{e}}y)$$	$$\sigma = \frac{3}{4}\sigma_{pt}\left[\eta(1+7\frac{\Delta}{s})\right.$$ $$\left. +4\frac{\Delta}{s}(1+\frac{\Delta}{s})\ln\frac{\Delta+s(1-\eta)}{\Delta+s(1+\eta)}\right]$$ $$\eta^2 = 1 - 2\frac{\Sigma}{s} + \left(\frac{\Delta}{s}\right)^2$$
$\gamma\gamma \to \tilde{e}\tilde{e}$		$$\frac{d\sigma}{dt} = \frac{4\pi\alpha^2}{s^2}\left[1 - \frac{2m_{\tilde{e}}^2 s(ut-m_{\tilde{e}}^4)}{(t-m_{\tilde{e}}^2)^2(u-m_{\tilde{e}}^2)^2}\right]$$ $$t = (p_{\tilde{e}} - p_\gamma)^2 = m_{\tilde{e}}^2 - \frac{s}{2}(1-\beta_{\tilde{e}}y)$$	$$\sigma = 3\sigma_{pt}\beta_{\tilde{e}}\left[2 - \beta_{\tilde{e}}^2 - \left(\frac{1-\beta_{\tilde{e}}^4}{2\beta_{\tilde{e}}}\right)\ln\frac{1+\beta_{\tilde{e}}}{1-\beta_{\tilde{e}}}\right]$$

Table II

Fig. Ia

Fig. Ib

Fig. Ic

Fig. Id

Fig. IIa

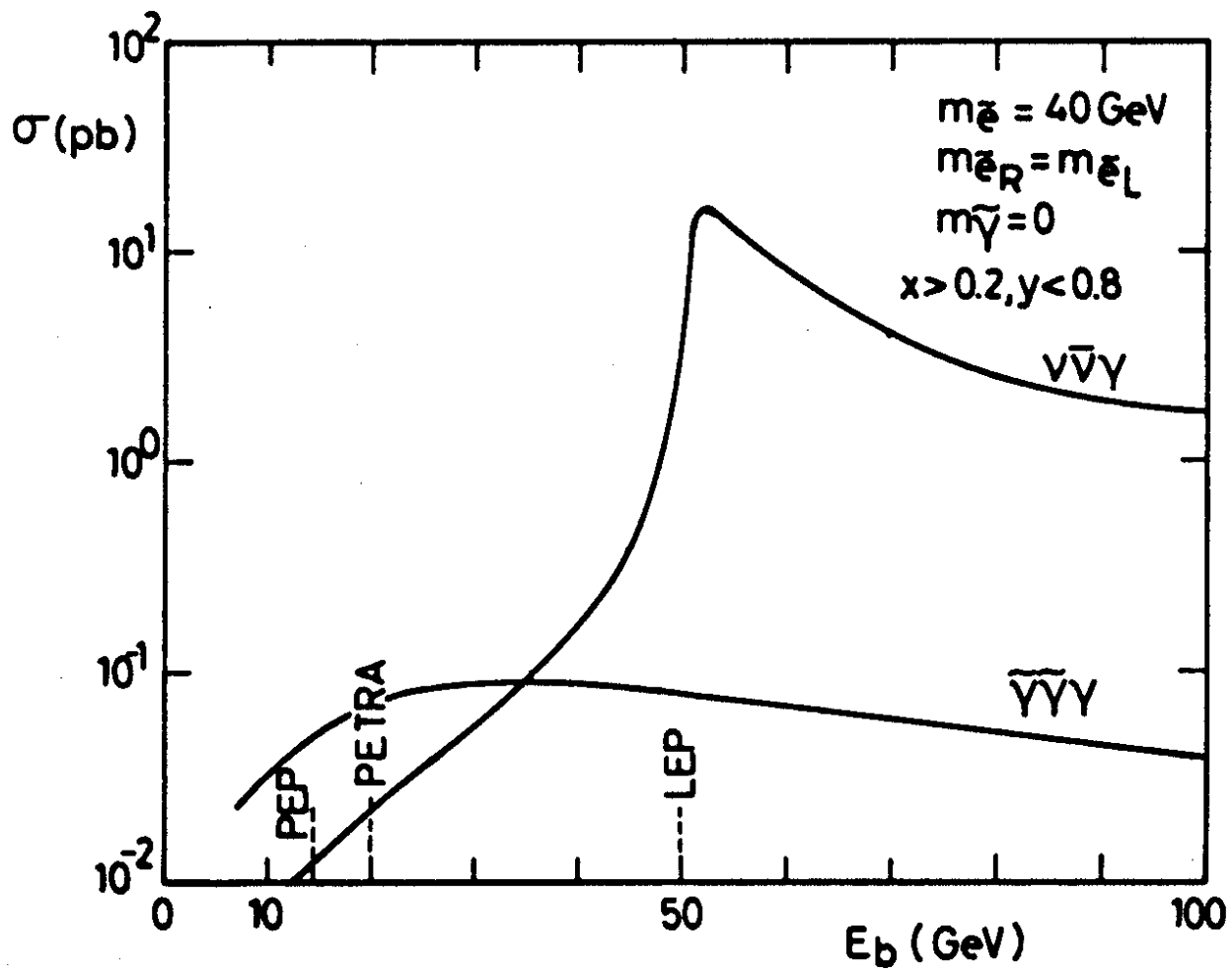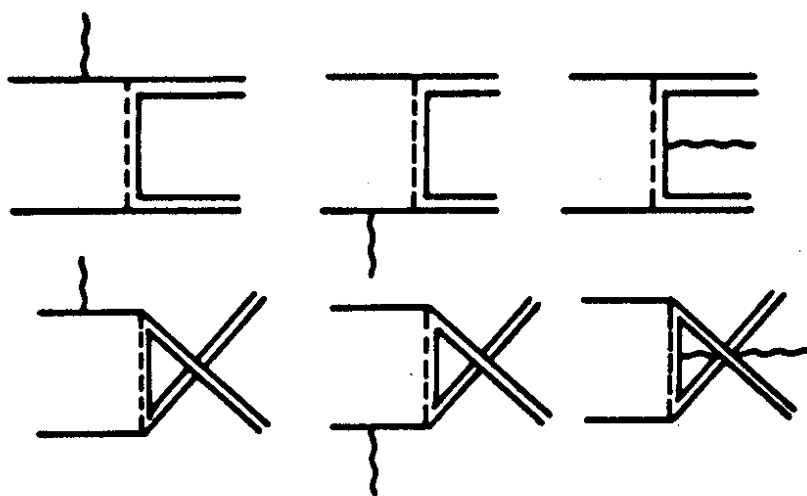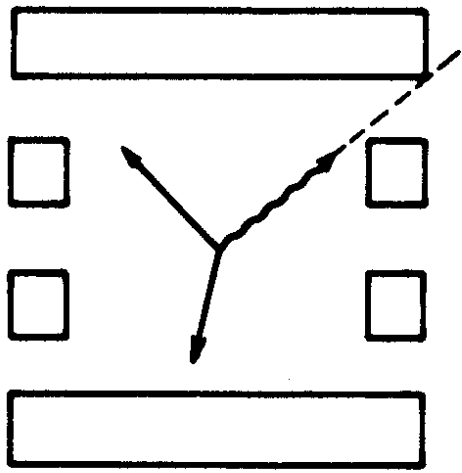Fig. IIc

Fig. IId

Fig. IIIa
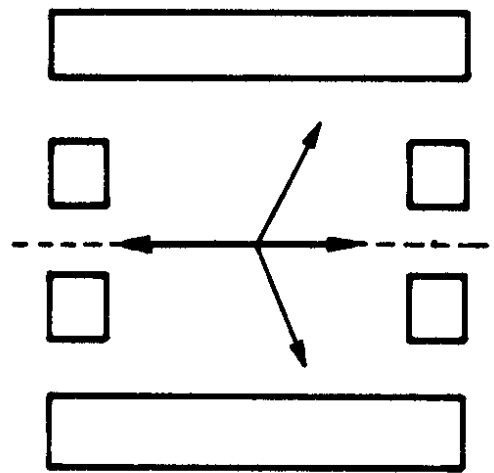
Fig. IIIb
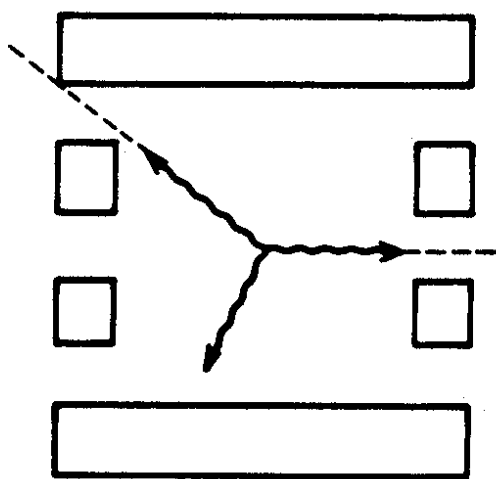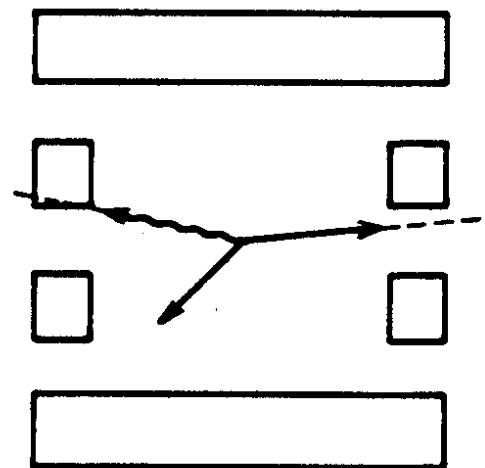
Fig. IIIc

Fig. IV a

Fig. IV b
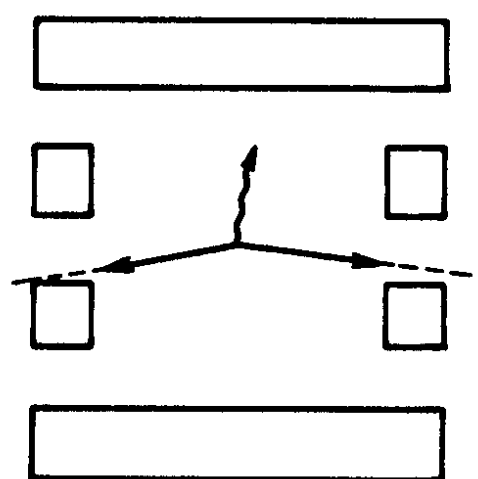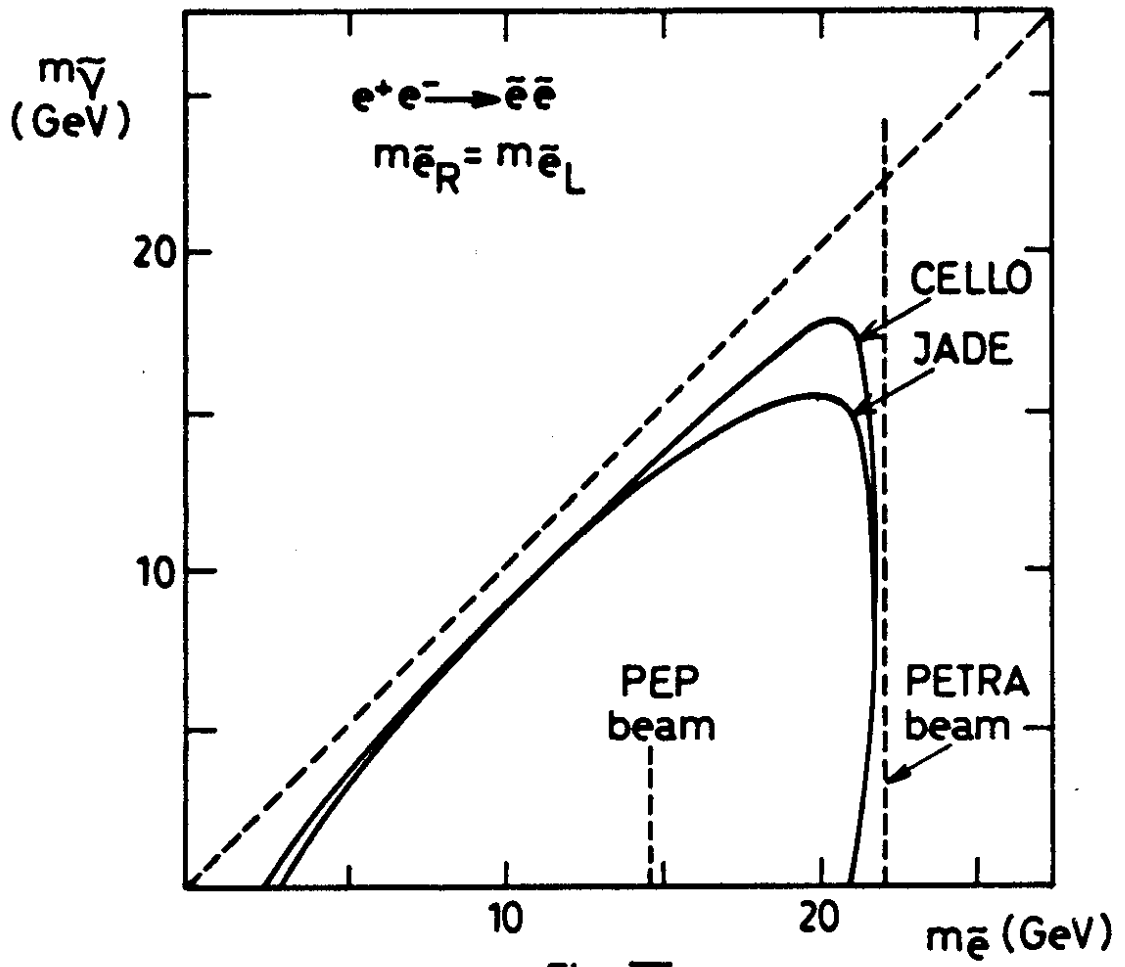
Fig. IVc
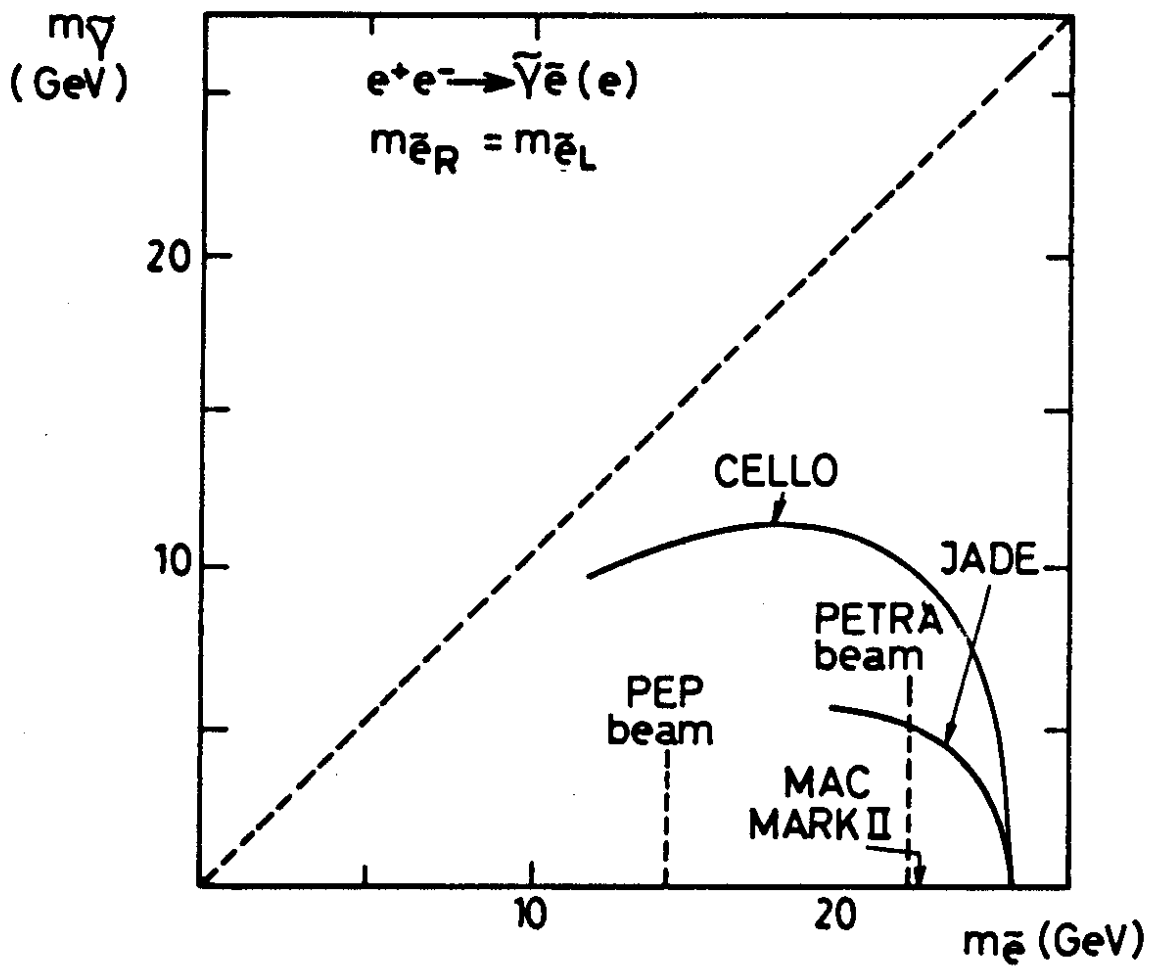
Fig. IVd

Fig. IV e

Fig. IV f
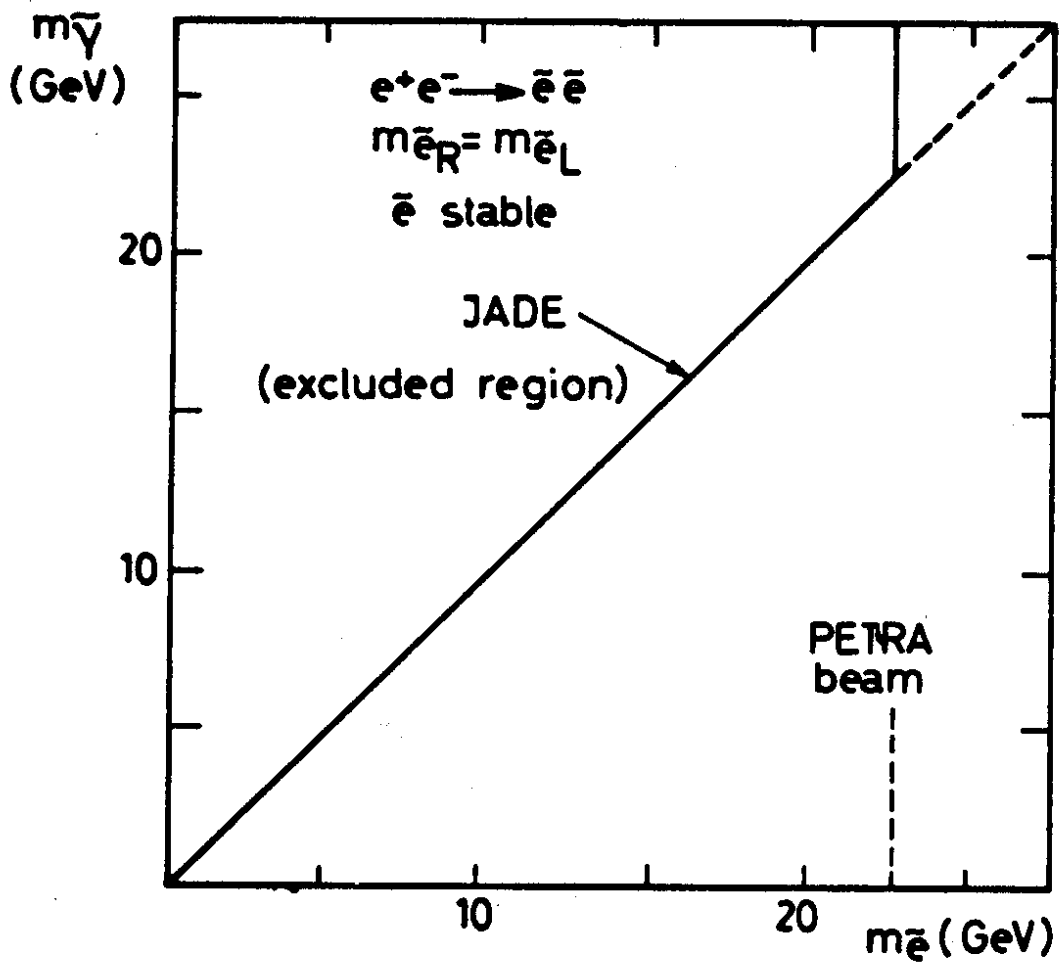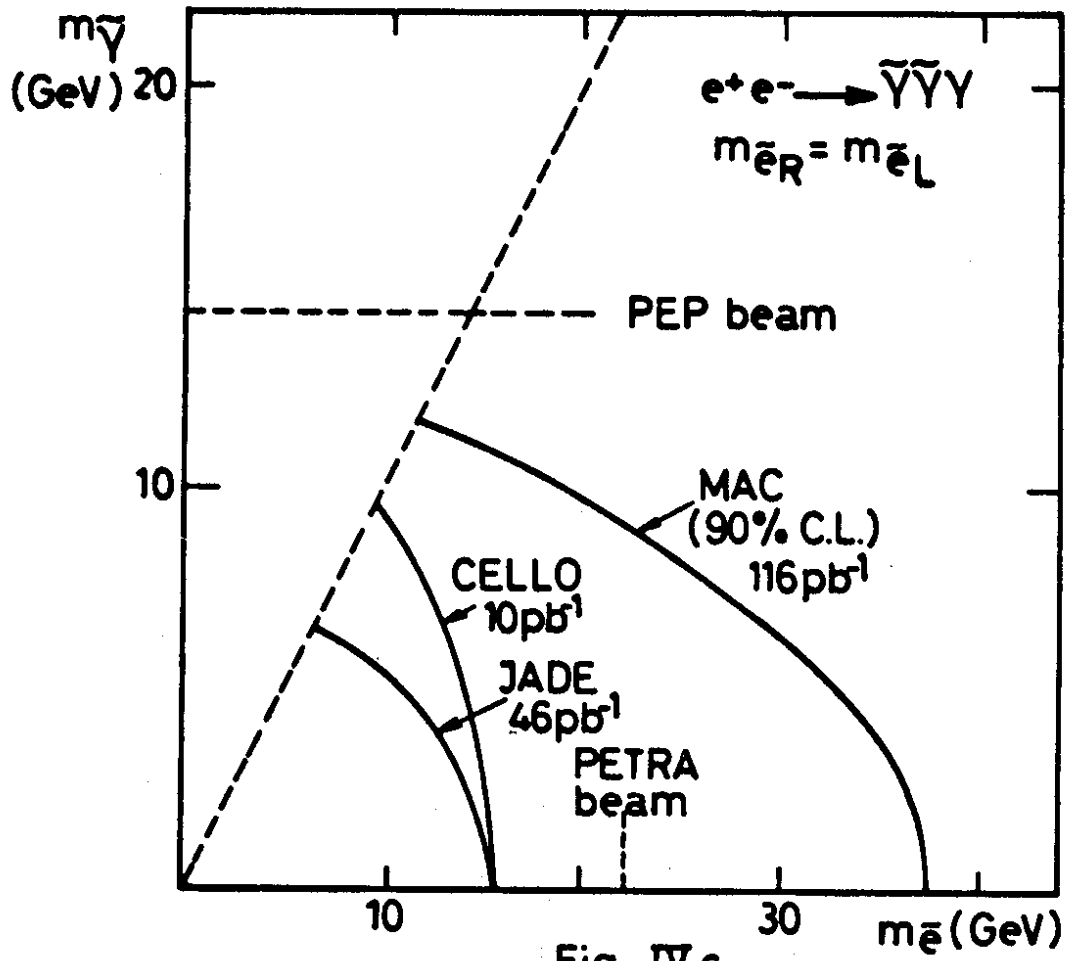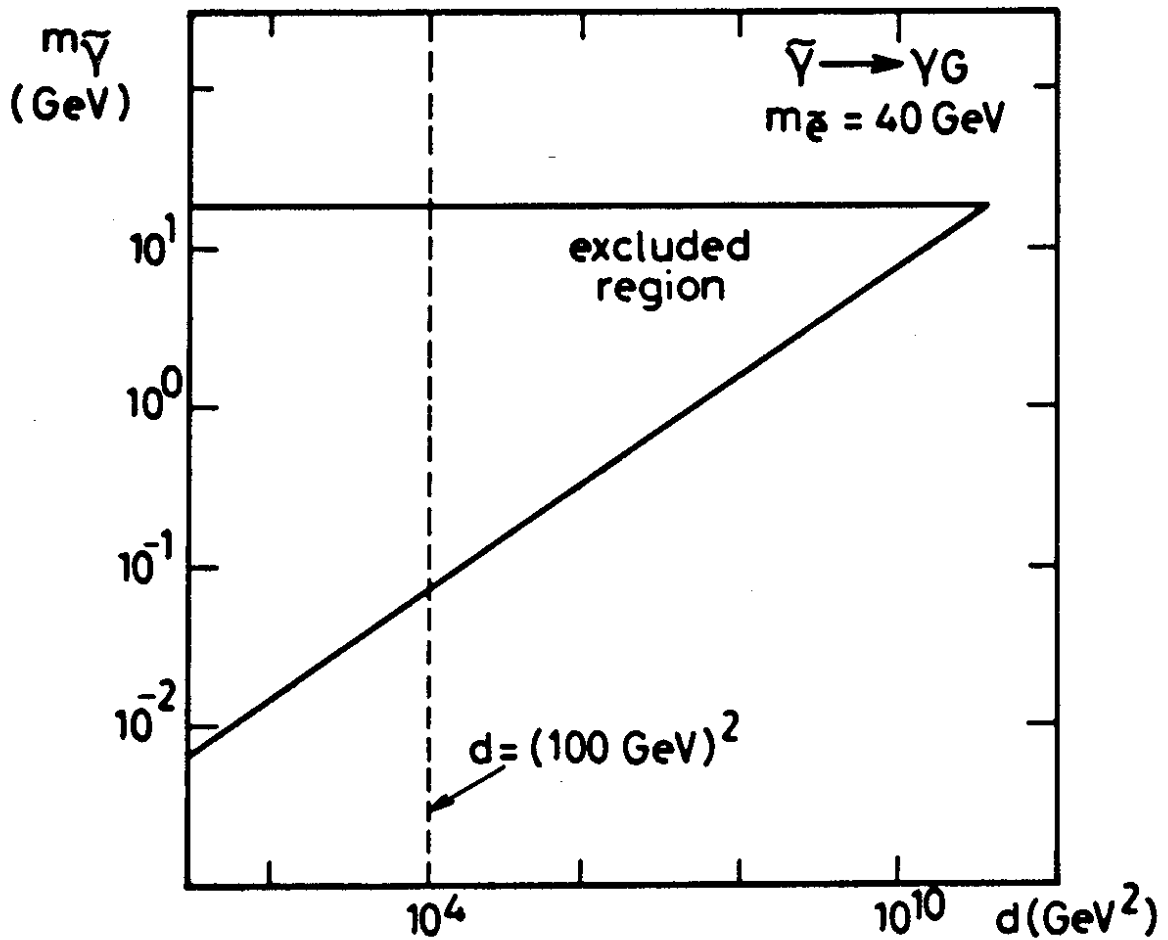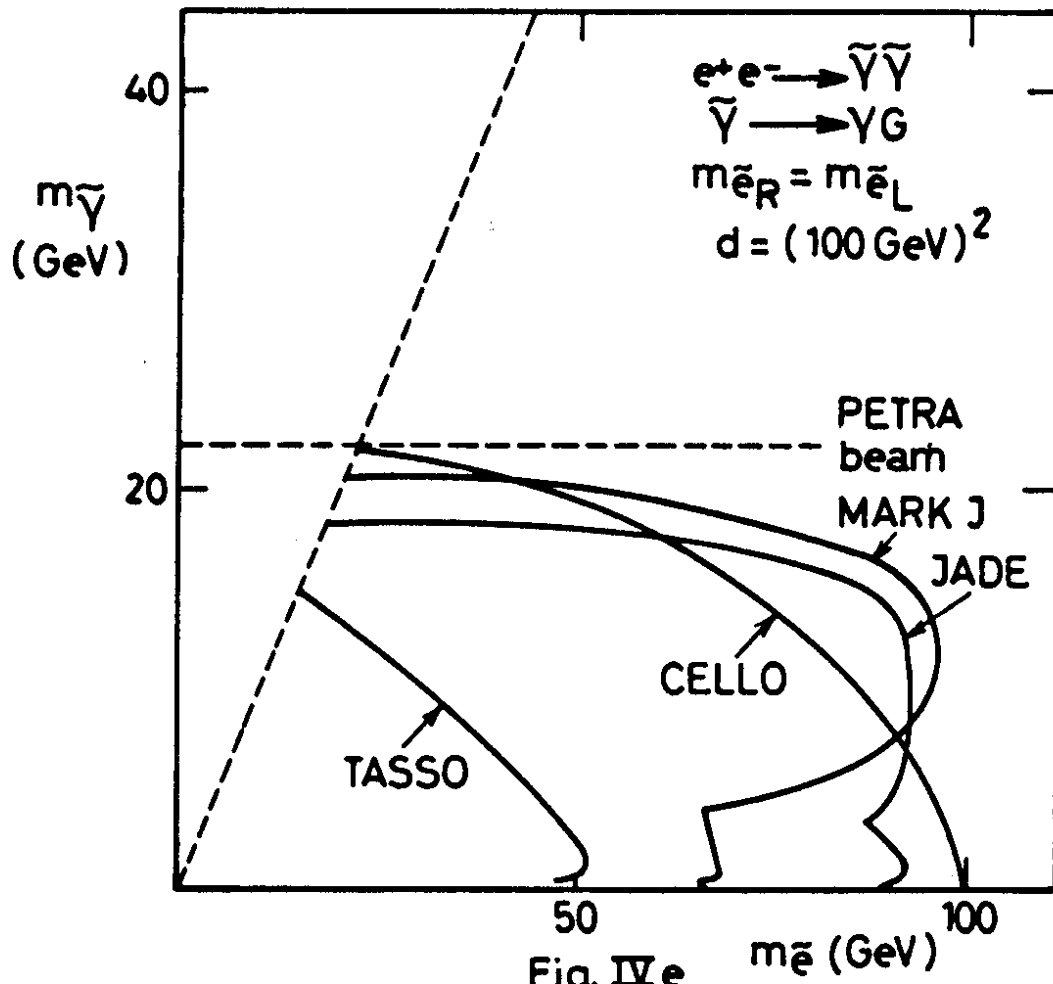
6-APPENDIX

In this appendix we derive angular distributions and cross-sections for the processes :

$$e^+e^- \rightarrow \tilde{e}\tilde{e}$$
$$e^+e^- \rightarrow \tilde{\gamma}\tilde{\gamma}$$
$$\gamma e \rightarrow \tilde{\gamma}\tilde{e}$$
$$\gamma\gamma \rightarrow \tilde{e}\tilde{e}$$

The interaction Lagrangian between scalar electrons and photinos is :
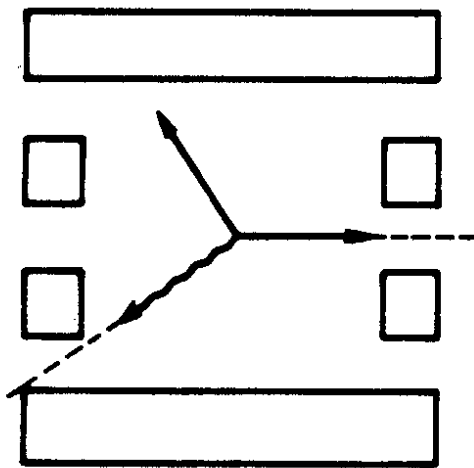
$$\sqrt{2}\{\tilde{e}_L[e(\frac{1+\gamma_5}{2})\tilde{\gamma}] + \tilde{e}_R[e(\frac{1-\gamma_5}{2})\tilde{\gamma}]\} + h.c.$$

The scalar electron has also electromagnetic interaction as any other scalar charged particle, adding the following piece to the Lagrangian :

$$-ieA_\mu(\tilde{e}^*\partial^\mu\tilde{e} - \tilde{e}\partial^\mu\tilde{e}^*) + e^2 A_\mu A^\mu \tilde{e}\tilde{e}^*$$

The corresponding Feynman diagrams are :

$$ie\sqrt{2}\left(\frac{1+\gamma_5}{2}\right)$$

$$ie\sqrt{2}\left(\frac{1-\gamma_5}{2}\right)$$

$$-ie(k+k')^\mu$$

$$2! \; ie^2 g^{\mu\nu}$$

18

$\underline{e^+e^- \to \tilde{e}\tilde{e}}$

The amplitude for the process $\tilde{e}_R^+\tilde{e}_R^-$, for example, is given by diagrams in figure A1. Its value is $T = T_1 + T_2$ where :

$$T_1 = \bar{v}_{p'}\left(ie\sqrt{2}\frac{1-\gamma_5}{2}\right)\frac{i}{\not{p}-\not{k}-m_{\tilde{\gamma}}}\left(ie\sqrt{2}\frac{1+\gamma_5}{2}\right)u_p = \frac{2ie^2}{t-m_{\tilde{\gamma}}^2}\bar{v}_{p'}\;\not{k}\left(\frac{1+\gamma_5}{2}\right)u_p$$

$$T_2 = \bar{v}_{p'}\left(-ie\gamma^\mu\right)u_p\frac{-i}{(p+p')^2}[-ie(k-k')_\mu] = \frac{2ie^2}{s}\bar{v}_{p'}\;\not{k}u_p$$

For the calculation of T_1 we used $\left(\frac{1\pm\gamma_5}{2}\right)^2 = \left(\frac{1\pm\gamma_5}{2}\right)$ but $\left(\frac{1-\gamma_5}{2}\right)\left(\frac{1+\gamma_5}{2}\right) = 0$, and also $\not{p}u_p = 0$; for the calculation of T_2 we used : $k-k' = 2k-p-p'$ and $m_e = 0$. The amplitude for $\tilde{e}_L^+\tilde{e}_L^-$ can be obtained by the exchange of $\frac{1\pm\gamma_5}{2}$ and $\frac{1\mp\gamma_5}{2}$; concerning the production of $\tilde{e}_R\tilde{e}_L$, the only amplitude is T_1 which becomes now :

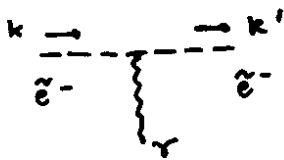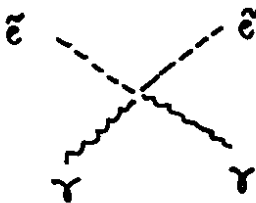$$T_1 = \bar{v}_{p'}\left(ie\sqrt{2}\frac{1\pm\gamma_5}{2}\right)\frac{i}{\not{p}-\not{k}-m_{\tilde{\gamma}}}\left(ie\sqrt{2}\frac{1\pm\gamma_5}{2}\right)u_p = -\frac{2ie^2}{t-m_{\tilde{\gamma}}^2}\bar{v}_{p'}\left(\frac{1\pm\gamma_5}{2}\right)m_{\tilde{\gamma}}u_p$$

where the projector $\frac{1\pm\gamma_5}{2}$ properties have been used again. Once we sum over polarisations and make the mean over initial states the squared amplitudes become:

$$\overline{|T_1|^2} = \frac{1}{4}\frac{4e^4}{(t-m_{\tilde{\gamma}}^2)^2}\sum_{pol}\bar{v}_{p'}\;\not{k}\left(\frac{1+\gamma_5}{2}\right)u_p\bar{u}_p\left(\frac{1-\gamma_5}{2}\right)\not{k}v_{p'}$$

$$= \frac{e^4}{(t-m_{\tilde{\gamma}}^2)^2}Tr\left[\not{k}\left(\frac{1+\gamma_5}{2}\right)\frac{\not{p}}{2m_e}\left(\frac{1-\gamma_5}{2}\right)\not{k}\frac{\not{p'}}{2m_e}\right]$$

$$= \frac{e^4}{(t-m_{\tilde{\gamma}}^2)^2}\frac{1}{8m_e^2}Tr(\not{k}\;\not{p}\;\not{k}\;\not{p'}) = \frac{e^4}{2m_e^2(t-m_{\tilde{\gamma}}^2)^2}[2(kp)(kp')-k^2pp']$$

The γ_5 term gives no contribution since one cannot find 4 independent fourvectors.

$$\left(\quad \text{for the case } \tilde{e}_R\tilde{e}_L \text{ we have} \quad \overline{|T_1|^2} = \frac{e^4}{(t-m_{\tilde{\gamma}}^2)^2}\frac{m_{\tilde{\gamma}}^2}{8m_e^2}Tr(\not{p}\;\not{p'}) = \frac{e^4 m_{\tilde{\gamma}}^2 pp'}{2m_e^2(t-m_{\tilde{\gamma}}^2)^2} \quad\right)$$

$$\overline{|T_2|^2} = \frac{1}{4}\frac{4e^4}{s^2}\sum_{pol}\bar{v}_{p'}\;\not{k}u_p\bar{u}_p\;\not{k}v_{p'} = \frac{e^4}{s^2}Tr\left(\frac{\not{p'}}{2m_e}\;\not{k}\frac{\not{p}}{2m_e}\;\not{k}\right)$$

$$= \frac{e^4}{m_e^2 s}[2(kp)(kp')-k^2pp']$$

$$2\overline{ReT_1T_2^*} = 2\frac{1}{4}\frac{4e^4}{s(t-m_{\tilde{\gamma}}^2)}\sum_{pol}\bar{v}_{p'}\;\not{k}\frac{1+\gamma_5}{2}u_p\bar{u}_p\;\not{k}v_{p'}$$

$$= \frac{2e^4}{s(t-m_{\tilde{\gamma}}^2)}Tr\left[\not{k}\frac{1+\gamma_5}{2}\frac{\not{p}}{2m_e}\;\not{k}\frac{\not{p'}}{2m_e}\right]$$

$$= \frac{e^4}{s(t-m_{\tilde{\gamma}}^2)}\frac{1}{4m_e^2}Tr(\not{k}\;\not{p}\;\not{k}\;\not{p'}) = \frac{e^4}{s(t-m_{\tilde{\gamma}}^2)m_e^2}[2(kp)(kp')-k^2pp']$$

Taking into account that $\tilde{e}_R$ and $\tilde{e}_L$ give equal contribution and including $e_R^+\tilde{e}_L^-$ and $\tilde{e}_R^+\tilde{e}_L^-$ productions, the total amplitude becomes :

$$\overline{|T|^2} = 2\frac{e^4}{2m_e^2}\left\{\left[\frac{1}{(t-m_{\tilde{\gamma}}^2)^2}+\frac{2}{s^2}+\frac{2}{s(t-m_{\tilde{\gamma}}^2)}\right]\left[2(kp)(kp')-k^2pp'\right]+\frac{m_{\tilde{\gamma}}^2 pp'}{(t-m_{\tilde{\gamma}}^2)^2}\right\}$$

Of course we assumed $m_{\tilde{e}_R} = m_{\tilde{e}_L}$. Using the relations :

$$kp = \frac{1}{2}(m_{\tilde{e}}^2-t)\qquad kp' = \frac{1}{2}(m_{\tilde{e}}^2-u)\qquad pp' = \frac{1}{2}s$$

19

we find :

$$\overline{|T|^2} = \frac{e^4}{2m_{\tilde{e}}^2}\left\{\left[1 + (1 + \frac{s}{t - m_{\tilde{\gamma}}^2})^2\right]\left[\frac{(m_{\tilde{e}}^2 - t)(m_{\tilde{e}}^2 - u)}{s^2} - \frac{m_{\tilde{e}}^2}{s}\right] + \frac{sm_{\tilde{\gamma}}^2}{(t - m_{\tilde{\gamma}}^2)^2}\right\}$$

$$= \frac{e^4}{2m_{\tilde{e}}^2}\left\{\left[1 + (1 + \frac{s}{t - m_{\tilde{\gamma}}^2})^2\right]\left[\frac{ut - m_{\tilde{e}}^4}{s^2}\right] + \frac{sm_{\tilde{\gamma}}^2}{(t - m_{\tilde{\gamma}}^2)^2}\right\}$$

The angular distribution is :

$$\boxed{\frac{d\sigma}{dt} = \frac{m_{\tilde{e}}^2}{4\pi s^2}\overline{|T|^2} = \frac{2\pi\alpha^2}{s^2}\left\{\left[1 + (1 + \frac{s}{t - m_{\tilde{\gamma}}^2})^2\right]\left[\frac{ut - m_{\tilde{e}}^4}{s^2}\right] + \frac{sm_{\tilde{\gamma}}^2}{(t - m_{\tilde{\gamma}}^2)^2}\right\}}$$

In terms of $y = \cos\theta$ and using the center of mass relations :

$$t = m_{\tilde{e}}^2 - \frac{s}{2}(1 - \beta_{\tilde{e}}y) \qquad u = m_{\tilde{e}}^2 - \frac{s}{2}(1 + \beta_{\tilde{e}}y)$$

we find : $\frac{d\sigma}{dy} = \beta_{\tilde{e}}^3\frac{\pi\alpha^2}{4s}\left\{\left[1 + (1 - \frac{4}{1 - 2\beta_{\tilde{e}}y + \beta_{\tilde{e}}^2 + \delta_{\tilde{\gamma}}^2})^2\right](1 - y^2) + \frac{16\delta_{\tilde{\gamma}}^2/\beta_{\tilde{e}}^2}{(1 - 2\beta_{\tilde{e}}y + \beta_{\tilde{e}}^2 + \delta_{\tilde{\gamma}}^2)^2}\right\}$

where $\beta_{\tilde{e}} = \sqrt{1 - \frac{4m_{\tilde{e}}^2}{s}}$ y $\delta_{\tilde{\gamma}}^2 = 4m_{\tilde{\gamma}}^2/s$. In order to obtain the total cross-section we can write :

$$\frac{d\sigma}{dy} = \frac{\pi\alpha^2}{4s}2\beta_{\tilde{e}}^3[1 - y^2 - b\frac{1 - y^2}{1 - ay} + c\frac{1 - y^2}{(1 - ay)^2} + d\frac{1}{(1 - ay)^2}]$$

with $a = \frac{2\beta_{\tilde{e}}}{1 + \beta_{\tilde{e}}^2 + \delta_{\tilde{\gamma}}^2}, b = \frac{4}{1 + \beta_{\tilde{e}}^2 + \delta_{\tilde{\gamma}}^2}, c = \frac{8}{(1 + \beta_{\tilde{e}}^2 + \delta_{\tilde{\gamma}}^2)^2}, d = \frac{8\delta_{\tilde{\gamma}}^2/\beta_{\tilde{e}}^2}{(1 + \beta_{\tilde{e}}^2 + \delta_{\tilde{\gamma}}^2)^2}$

Then the total cross-section is $\sigma = F(1) - F(-1)$ with :

$$F(y) = \int_0^y \frac{d\sigma}{dy}dy = \frac{\pi\alpha^2}{4s}2\beta_{\tilde{e}}^3[f_0(y) - bf_1(y) + cf_2(y) + df_3(y)]$$

$$f_0(y) = \int_0^y (1 - y^2)dy = y - \frac{1}{3}y^3$$

$$f_1(y) = \int_0^y \frac{1 - y^2}{1 - ay}dy = \frac{1}{a}[\frac{y}{a} + \frac{y^2}{2} - (1 - \frac{1}{a^2})\ln(1 - ay)]$$

$$f_2(y) = \int_0^y \frac{1 - y^2}{(1 - ay)^2}dy = -\frac{1}{a^2}[\frac{1 - a^2}{1 - ay}y + y + \frac{2}{a}\ln(1 - ay)]$$

$$f_3(y) = \int_0^y \frac{1}{(1 - ay)^2}dy = \frac{y}{1 - ay}$$

After some calculations we find :

$$\sigma = \frac{\pi\alpha^2}{4s}2\beta_{\tilde{e}}^3\left\{\frac{4}{3} - \frac{b}{a}[\frac{2}{a} - (1 - \frac{1}{a^2})\ln\frac{1 - a}{1 + a}] - \frac{c}{a^2}[4 + \frac{2}{a}\ln\frac{1 - a}{1 + a}] + \frac{2d}{1 - a^2}\right\}$$

$$= \frac{\pi\alpha^2}{4s}\beta_{\tilde{e}}\left\{-(20 + \frac{4}{3}\beta_{\tilde{e}}^2 + 4\delta_{\tilde{\gamma}}^2) + \frac{1}{\beta_{\tilde{e}}}[4(1 + \delta_{\tilde{\gamma}}^2) + (1 + \beta_{\tilde{e}}^2 + \delta_{\tilde{\gamma}}^2)^2]\ln\frac{(1 + \beta_{\tilde{e}})^2 + \delta_{\tilde{\gamma}}^2}{(1 - \beta_{\tilde{e}})^2 + \delta_{\tilde{\gamma}}^2} + \frac{32\delta_{\tilde{\gamma}}^2}{(1 + \beta_{\tilde{e}}^2 + \delta_{\tilde{\gamma}}^2)^2 - 4\beta_{\tilde{e}}^2}\right\}$$

or in terms of $\Delta = m_{\tilde{e}}^2 - m_{\tilde{\gamma}}^2$:

$$\boxed{\sigma = \frac{\pi\alpha^2}{s}\beta_{\tilde{e}}\left\{-(5 + \frac{\beta_{\tilde{e}}^2}{3} + 4\frac{m_{\tilde{\gamma}}^2}{s}) + \frac{8m_{\tilde{\gamma}}^2/s}{(1 - 2\frac{\Delta}{s})^2 - \beta_{\tilde{e}}^2} + \frac{1}{\beta_{\tilde{e}}}[1 + \frac{4m_{\tilde{\gamma}}^2}{s} + (1 - 2\frac{\Delta}{s})^2]\ln\frac{\Delta - \frac{s}{2}(1 + \beta_{\tilde{e}})}{\Delta - \frac{s}{2}(1 - \beta_{\tilde{e}})}\right\}}$$

20

$\underline{e^+e^- \to \tilde{\gamma}\tilde{\gamma}}$

The two diagrams contributing to this process are shown in figure A2; the total amplitude is $T = T_1 - T_2$ where, for an $\tilde{e}_L$ exchange :

$$T_1 = \bar{u}_q [ie\sqrt{2}\frac{1-\gamma_5}{2}]u_p[\frac{i}{t-m_{\tilde{e}}^2}]\bar{v}_{p'}[ie\sqrt{2}\frac{1+\gamma_5}{2}]v_{q'}$$

$$T_2 = \bar{u}_{q'}[ie\sqrt{2}\frac{1-\gamma_5}{2}]u_p[\frac{i}{u-m_{\tilde{e}}^2}]\bar{v}_{p'}[ie\sqrt{2}\frac{1+\gamma_5}{2}]v_q$$

For $\tilde{e}_R$ one can change γ_5 by $-\gamma_5$; the $-$ sign between T_1 and T_2 is due to the fermionic nature of the produced photinos. The squared and averaged amplitude is $\overline{|T|^2} = \overline{|T_1|^2} + \overline{|T_2|^2} - 2\overline{ReT_1T_2^*}$ with :

$$\overline{|T_1|^2} = \frac{1}{4}\frac{4e^4}{(t-m_{\tilde{e}}^2)^2}\sum_{pol}\bar{u}_q\frac{1-\gamma_5}{2}u_p\bar{u}_p\frac{1+\gamma_5}{2}u_q\bar{v}_{p'}\frac{1+\gamma_5}{2}v_{q'}\bar{v}_{q'}\frac{1-\gamma_5}{2}v_{p'}$$

$$= \frac{e^4}{(t-m_{\tilde{e}}^2)^2}Tr[\frac{1-\gamma_5}{2}\frac{\not{p}}{2m_e}\frac{1+\gamma_5}{2}\frac{\not{q}+m_{\tilde{\gamma}}}{2m_{\tilde{\gamma}}}]Tr[\frac{1+\gamma_5}{2}\frac{\not{q}'-m_{\tilde{\gamma}}}{2m_{\tilde{\gamma}}}\frac{1-\gamma_5}{2}\frac{\not{p}'}{2m_e}]$$

$$= \frac{e^4}{(t-m_{\tilde{e}}^2)^2}\frac{1}{16m_e^2m_{\tilde{\gamma}}^2}Tr[\frac{1}{2}\not{p}\not{q}]Tr[\frac{1}{2}\not{q}'\not{p}']$$

$$= \frac{1}{4}\frac{e^4}{m_e^2m_{\tilde{\gamma}}^2}\frac{(pq)(p'q')}{(t-m_{\tilde{e}}^2)^2}$$

$$\overline{|T_2|^2} = \frac{1}{4}\frac{e^4}{m_e^2m_{\tilde{\gamma}}^2}\frac{(pq')(p'q)}{(u-m_{\tilde{e}}^2)^2} \quad \text{(by exchange } q \leftrightarrow q')$$

$$2\overline{ReT_1T_2^*} = \frac{1}{2}\frac{4e^4}{(t-m_{\tilde{e}}^2)(u-m_{\tilde{e}}^2)}\sum_{pol}\bar{u}_q\frac{1-\gamma_5}{2}u_p\bar{u}_p\frac{1+\gamma_5}{2}u_{q'}\bar{v}_q\frac{1-\gamma_5}{2}v_{p'}\bar{v}_{p'}\frac{1+\gamma_5}{2}v_{q'}$$

$$= \frac{1}{2}\frac{4e^4}{(t-m_{\tilde{e}}^2)(u-m_{\tilde{e}}^2)}\sum_{pol\tilde{\gamma}}[\bar{u}_q\frac{1-\gamma_5}{2}\frac{\not{p}}{2m_e}u_{q'}][\bar{v}_q\frac{\not{p}'}{2m_e}\frac{1+\gamma_5}{2}v_{q'}]$$

We need at this point the following transformation :

$$\bar{v}_q\frac{\not{p}'}{2m_e}\frac{1+\gamma_5}{2}v_{q'} = \left[\bar{v}_q\frac{\not{p}'}{2m_e}\frac{1+\gamma_5}{2}v_{q'}\right]^T = v_{q'}^T\left(\frac{1+\gamma_5}{2}\right)^T\left(\frac{\not{p}'}{2m_e}\right)^T\bar{v}_q^T$$

$$= \bar{u}_{q'}C\left(1+\frac{C^{-1}\gamma_5C}{2}\right)\frac{C^{-1}\not{p}'C}{2m_e}C^{-1}u_q = \bar{u}_{q'}\frac{1+\gamma_5}{2}\frac{\not{p}'}{2m_e}u_q$$

where use has been made of :

$$v = Cu^T \qquad u = Cv^T \qquad v^T = -\bar{u}C \qquad u^T = -\bar{v}C$$

and the following C matrix properties :

$$C^+ = C^{-1} \qquad C^T = -C \qquad C^{-1}\gamma C = -\gamma^T \qquad C^{-1}\gamma_5C = \gamma_5^T$$

Then :

$$2\overline{ReT_1T_2^*} = \frac{1}{2}\frac{4e^4}{(t-m_{\tilde{e}}^2)(u-m_{\tilde{e}}^2)}Tr[\frac{1-\gamma_5}{2}\frac{\not{p}}{2m_e}\frac{\not{q}'+m_{\tilde{\gamma}}}{2m_{\tilde{\gamma}}}\frac{1+\gamma_5}{2}\frac{\not{p}'}{2m_e}\frac{\not{q}+m_{\tilde{\gamma}}}{2m_{\tilde{\gamma}}}]$$

$$= \frac{1}{2}\frac{4e^4}{(t-m_{\tilde{e}}^2)(u-m_{\tilde{e}}^2)}Tr[\frac{1-\gamma_5}{2}\frac{\not{p}m_{\tilde{\gamma}}\not{p}'m_{\tilde{\gamma}}}{16m_e^2m_{\tilde{\gamma}}^2}]$$

$$= \frac{1}{4}\frac{e^4}{m_e^2m_{\tilde{\gamma}}^2}\frac{m_{\tilde{\gamma}}^2pp'}{(t-m_{\tilde{e}}^2)(u-m_{\tilde{e}}^2)}$$

The γ_5 terms do not contribute and then $\tilde{e}_R$ gives a similar amplitude; it's also easy to see that there is no interference between $\tilde{e}_R$ and $\tilde{e}_L$. Adding $\tilde{e}_R$ and $\tilde{e}_L$ contributions and assuming $m_{\tilde{e}_R} = m_{\tilde{e}_L}$, we find :

$$\overline{|T|^2} = 2\frac{e^4}{4m_e^2m_{\tilde{\gamma}}^2}\left[\frac{(pq)(p'q')}{(t-m_{\tilde{e}}^2)^2} + \frac{(pq')(p'q)}{(u-m_{\tilde{e}}^2)^2} - \frac{m_{\tilde{\gamma}}^2pp'}{(t-m_{\tilde{e}}^2)(u-m_{\tilde{e}}^2)}\right]$$

$$= \frac{2\pi^2\alpha^2}{m_e^2m_{\tilde{\gamma}}^2}\left[\frac{(t-m_{\tilde{\gamma}}^2)^2}{(t-m_{\tilde{e}}^2)^2} + \frac{(u-m_{\tilde{\gamma}}^2)^2}{(u-m_{\tilde{e}}^2)^2} - \frac{2m_{\tilde{\gamma}}^2s}{(t-m_{\tilde{e}}^2)(u-m_{\tilde{e}}^2)}\right]$$

21

and the angular distribution is :

$$\frac{d\sigma}{dt} = \frac{m_e^2 m_{\tilde{\gamma}}^2}{\pi s^2}\overline{|T|^2} = \frac{2\pi\alpha^2}{s^2}\left[\frac{(t-m_{\tilde{\gamma}}^2)^2}{(t-m_{\tilde{e}}^2)^2} + \frac{(u-m_{\tilde{\gamma}}^2)^2}{(u-m_{\tilde{e}}^2)^2} - \frac{2m_{\tilde{\gamma}}^2 s}{(t-m_{\tilde{e}}^2)(u-m_{\tilde{e}}^2)}\right]$$

As $\qquad t = m_{\tilde{\gamma}}^2 - \frac{s}{2}(1-\beta_{\tilde{\gamma}}y) \qquad u = m_{\tilde{\gamma}}^2 - \frac{s}{2}(1+\beta_{\tilde{\gamma}}y)$

we have in terms of $y = \cos\theta$, θ being the center-of-mass scattering angle :

$$\frac{d\sigma}{dy} = \frac{\pi\alpha^2}{s}\beta_{\tilde{\gamma}}\left\{\left[\frac{\frac{s}{2}(1-\beta_{\tilde{\gamma}}y)}{\Delta+\frac{s}{2}(1-\beta_{\tilde{\gamma}}y)}\right]^2 + \left[\frac{\frac{s}{2}(1+\beta_{\tilde{\gamma}}y)}{\Delta+\frac{s}{2}(1+\beta_{\tilde{\gamma}}y)}\right]^2 - \frac{2m_{\tilde{\gamma}}^2 s}{[\Delta+\frac{s}{2}(1-\beta_{\tilde{\gamma}}y)][\Delta+\frac{s}{2}(1+\beta_{\tilde{\gamma}}y)]}\right\}$$

with $\qquad \Delta = m_{\tilde{e}}^2 - m_{\tilde{\gamma}}^2 \qquad \beta_{\tilde{\gamma}} = \sqrt{1 - 4\frac{m_{\tilde{\gamma}}^2}{s}}$

In order to compute the total cross-section we observe that :

$$\left[\frac{t-m_{\tilde{\gamma}}^2}{t-m_{\tilde{e}}^2}\right]^2 = \left[1 + \frac{\Delta}{t-m_{\tilde{e}}^2}\right]^2 = 1 + \frac{2\Delta}{\tau} + \frac{\Delta^2}{\tau^2}$$

$$-\frac{2m_{\tilde{\gamma}}^2 s}{(t-m_{\tilde{e}}^2)(u-m_{\tilde{e}}^2)} = \frac{2m_{\tilde{\gamma}}^2 s}{s+2\Delta}\left[\frac{1}{\tau} + (t\leftrightarrow u)\right]$$

Where $\tau = t - m_{\tilde{e}}^2$. Then :

$$\sigma = \frac{1}{2!}2\frac{2\pi\alpha^2}{s^2}\int_{\tau_1}^{\tau_2} d\tau\left[1 + \frac{\Delta^2}{\tau^2} + (2\Delta + \frac{2m_{\tilde{\gamma}}^2 s}{s+2\Delta})\frac{1}{\tau}\right]$$

The $1/2!$ factor is due to the production of identical particles in the final state and an additional factor 2 to the u terms contribution.

$$\sigma = \frac{2\pi\alpha^2}{s^2}\left[(\tau_2 - \tau_1) - \Delta^2(\frac{1}{\tau_2} - \frac{1}{\tau_1}) + (2\Delta + \frac{2m_{\tilde{\gamma}}^2 s}{s+2\Delta})\ln\frac{\tau_2}{\tau_1}\right]$$

As $\qquad \tau_1 = t_1 - m_{\tilde{e}}^2 = -\Delta - \frac{s}{2}(1+\beta_{\tilde{\gamma}}) \qquad \tau_2 = t_2 - m_{\tilde{e}}^2 = -\Delta - \frac{s}{2}(1-\beta_{\tilde{\gamma}})$

we have $\qquad \tau_2 - \tau_1 = s\beta_{\tilde{\gamma}} \qquad$ and $\qquad \tau_1\tau_2 = \Delta^2 + sm_{\tilde{e}}^2 \qquad$, so :

$$\sigma = \frac{4\pi\alpha^2\beta_{\tilde{\gamma}}}{s}(\Delta^2 + \frac{s}{2}m_{\tilde{e}}^2)\left[\frac{1}{\Delta^2 + sm_{\tilde{e}}^2} - \frac{1}{s\beta_{\tilde{\gamma}}(\Delta + \frac{s}{2})}\ln\frac{\Delta + \frac{s}{2}(1+\beta_{\tilde{\gamma}})}{\Delta + \frac{s}{2}(1-\beta_{\tilde{\gamma}})}\right]$$

$e\gamma \rightarrow \tilde{e}\tilde{\gamma}$

The amplitude for this process is $T = T_1 + T_2$ where T_1 and T_2 correspond to the diagrams shown in figure A3; for $\tilde{e}_R$ production for example :

$$T_1 = \bar{u}_{p'}\left(ie\sqrt{2}\frac{1+\gamma_5}{2}\right)\frac{i}{t-m_{\tilde{e}}^2}[-ie(2k'-k)\epsilon]u_p = \frac{ie^2}{\sqrt{2}}\bar{u}_{p'}(1+\gamma_5)u_p\frac{(2k'-k)\epsilon}{t-m_{\tilde{e}}^2}$$

$$T_2 = \bar{u}_{p'}\left(ie\sqrt{2}\frac{1+\gamma_5}{2}\right)\frac{i}{\not{p}+\not{k}}(-ie\not{\epsilon})u_p = \frac{ie^2}{\sqrt{2}s}\bar{u}_{p'}(1+\gamma_5)(\not{p}+\not{k})\not{\epsilon}u_p$$

Where t is the square of the tranfered momentum between the scalar electron and the photon. The squared and averaged total amplitude is $\overline{|T|^2} = \overline{|T_1|^2} + \overline{|T_2|^2} + 2\overline{ReT_1T_2^*}$ where :

$$\overline{|T_1|^2} = \frac{1}{4}\sum_{pol}\frac{e^4}{2}\frac{[(2k'-k)\epsilon]^2}{(t-m_{\tilde{e}}^2)^2}\bar{u}_{p'}(1+\gamma_5)u_p\bar{u}_p(1-\gamma_5)u_{p'}$$

$$= -\frac{e^4}{8}\frac{(2k'-k)^2}{(t-m_{\tilde{e}}^2)^2}Tr[\frac{\not{p}'}{2m_{\tilde{\gamma}}}(1+\gamma_5)\frac{\not{p}}{2m_e}(1-\gamma_5)]$$

$$= -\frac{e^4(2k'-k)^2 pp'}{4m_e m_{\tilde{\gamma}}(t-m_{\tilde{e}}^2)^2} = -\frac{e^4}{4m_e m_{\tilde{\gamma}}}\frac{4(m_{\tilde{e}}^2-kk')pp'}{(t-m_{\tilde{e}}^2)^2}$$

$$\overline{|T_2|^2} = \frac{1}{4}\sum_{pol}\frac{e^4}{2s^2}\bar{u}_{p'}(1+\gamma_5)(\not{p}+\not{k})\not{\epsilon}u_p\bar{u}_p\not{\epsilon}(1+\gamma_5)(\not{p}+\not{k})u_{p'}$$

$$= \frac{e^4}{8s^2}\sum_{pol}Tr[(1+\gamma_5)(\not{p}+\not{k})\not{\epsilon}\frac{\not{p}}{2m_e}\not{\epsilon}(1+\gamma_5)(\not{p}+\not{k})\frac{\not{p}'}{2m_{\tilde{\gamma}}}]$$

$$= \frac{e^4}{8m_e m_{\tilde{\gamma}}s^2}Tr[(1+\gamma_5)(\not{p}+\not{k})\not{p}(\not{p}+\not{k})\not{p}']$$

$$= \frac{e^4}{8m_e m_{\tilde{\gamma}}s^2}Tr[(1+\gamma_5)\not{k}\not{p}\not{k}\not{p}'] = \frac{e^4}{4m_e m_{\tilde{\gamma}}}\frac{4(kp)(kp')}{s^2}$$

$$2\overline{ReT_1T_2^*} = 2\frac{1}{4}\sum_{pol}\frac{e^4}{2s}\bar{u}_{p'}(1+\gamma_5)(\not{p}+\not{k})\not{\epsilon}u_p\bar{u}_p(1-\gamma_5)u_{p'}\frac{(2k'-k)\epsilon}{t-m_{\tilde{e}}^2}$$

$$= \frac{e^4}{4s}\sum_{pol}Tr[\frac{\not{p}'}{2m_{\tilde{\gamma}}}(1+\gamma_5)(\not{p}+\not{k})\not{\epsilon}\frac{\not{p}}{2m_e}(1-\gamma_5)]\frac{(2k'-k)\epsilon}{t-m_{\tilde{e}}^2}$$

$$= -\frac{e^4}{8(t-m_{\tilde{e}}^2)m_e m_{\tilde{\gamma}}s}Tr[\not{p}'(\not{p}+\not{k})(2\not{k}'-\not{k})\not{p}]$$

$$= -\frac{e^4}{4m_e m_{\tilde{\gamma}}}\frac{4pp'(kp-m_{\tilde{\gamma}}^2-2k'p')+4m_{\tilde{\gamma}}^2k'p}{s(t-m_{\tilde{e}}^2)}$$

We note again that the amplitudes are not γ_5 depending and then $\tilde{e}_R$ and $\tilde{e}_L$ give equal contributions to the total amplitude that will be obtained multiplying by 2 :

$$\overline{|T|^2} = \frac{2e^4}{4m_e m_{\tilde{\gamma}}}\left[\frac{4(kp)(kp')}{s^2} - \frac{4(m_{\tilde{e}}^2-kk')pp'}{(t-m_{\tilde{e}}^2)^2} - \frac{4pp'(kp-m_{\tilde{\gamma}}^2-2k'p')+4m_{\tilde{\gamma}}^2k'p}{s(t-m_{\tilde{e}}^2)}\right]$$

Using the relations :

$$kp = \frac{1}{2}s \qquad kk' = \frac{1}{2}(m_{\tilde{e}}^2-t) \qquad kp' = \frac{1}{2}(m_{\tilde{\gamma}}^2-u)$$

$$k'p' = \frac{1}{2}(s-m_{\tilde{e}}^2-m_{\tilde{\gamma}}^2) \qquad pp' = \frac{1}{2}(m_{\tilde{\gamma}}^2-t) \qquad pk' = \frac{1}{2}(m_{\tilde{e}}^2-u)$$

we have : $\overline{|T|^2} = \frac{2e^4}{4m_e m_{\tilde{\gamma}}}\left[\frac{m_{\tilde{\gamma}}^2-u}{s} + \frac{(t-m_{\tilde{\gamma}}^2)(t+m_{\tilde{e}}^2)}{(t-m_{\tilde{e}}^2)^2} - \frac{(t-m_{\tilde{\gamma}}^2)(s-2\Delta)+2sm_{\tilde{\gamma}}^2}{s(t-m_{\tilde{e}}^2)}\right]$

where $\Delta = m_{\tilde{e}}^2 - m_{\tilde{\gamma}}^2$; the angular distribution is :

$$\boxed{\frac{d\sigma}{dt} = \frac{m_e m_{\tilde{\gamma}}}{4\pi s^2}\overline{|T|^2} = \frac{2\pi\alpha^2}{s^2}\left[\frac{m_{\tilde{\gamma}}^2-u}{s} + \frac{(t-m_{\tilde{\gamma}}^2)(t+m_{\tilde{e}}^2)}{(t-m_{\tilde{e}}^2)^2} - \frac{(t-m_{\tilde{\gamma}}^2)(s-2\Delta)+2sm_{\tilde{\gamma}}^2}{s(t-m_{\tilde{e}}^2)}\right]}$$

23

In order to integrate this expression we define $\tau = t - m_{\tilde{e}}^2$; then :

$$\frac{d\sigma}{d\tau} = \frac{2\pi\alpha^2}{s^2}\left[\frac{s+\tau}{s} + \frac{(\tau+\Delta)(\tau+2m_{\tilde{e}}^2)}{\tau^2} - \frac{(\tau+\Delta)(s-2\Delta)+2sm_{\tilde{\gamma}}^2}{s\tau}\right]$$

$$= \frac{2\pi\alpha^2}{s^2}\left[\frac{\tau}{s} + 1 + \frac{2\Delta}{s} + 2m_{\tilde{e}}^2\frac{\Delta}{\tau^2} + \frac{2\Delta}{\tau}(1+\frac{\Delta}{s})\right]$$

$$\sigma = \frac{2\pi\alpha^2}{s}\left[\frac{\tau^2}{2s^2} + (1+2\frac{\Delta}{s})\frac{\tau}{s} - \frac{2m_{\tilde{e}}^2}{\tau}\frac{\Delta}{s} + 2\frac{\Delta}{s}(1+\frac{\Delta}{s})\ln\tau\right]_{\tau_1}^{\tau_2}$$

$$= \frac{\pi\alpha^2}{s}\left\{\frac{\tau_2-\tau_1}{s}\left[\frac{\tau_2+\tau_1}{s} + 2(1+2\frac{\Delta}{s}) + \frac{4\Delta m_{\tilde{e}}^2}{\tau_1\tau_2}\right] + 4\frac{\Delta}{s}(1+\frac{\Delta}{s})\ln\frac{\tau_2}{\tau_1}\right\}$$

As $\tau = t - m_{\tilde{e}}^2 = -\frac{s}{2}\frac{E_{\tilde{e}}}{E_b}\left(1-\beta_{\tilde{e}}y\right)$ in the center-of-mass frame, the integration limits are :

$$\tau_1 = -\frac{s}{2}\frac{E_{\tilde{e}}}{E_b}(1+\beta_{\tilde{e}}) \qquad \tau_2 = -\frac{s}{2}\frac{E_{\tilde{e}}}{E_b}(1-\beta_{\tilde{e}})$$

But : $\dfrac{E_{\tilde{e}}}{E_b} = 1 + \dfrac{\Delta}{s}$ then $\beta_{\tilde{e}} = \sqrt{1 - \dfrac{m_{\tilde{e}}^2}{E_{\tilde{e}}^2}} = \dfrac{1}{1+\frac{\Delta}{s}}\sqrt{(1+\frac{\Delta}{s})^2 - 4\frac{m_{\tilde{e}}^2}{s}} = \dfrac{\eta}{1+\frac{\Delta}{s}}$

with $\eta = \sqrt{1 - 2\dfrac{\Sigma}{s} + (\dfrac{\Delta}{s})^2}$ and $\Sigma = m_{\tilde{e}}^2 + m_{\tilde{\gamma}}^2$ then :

$$\frac{\tau_2}{\tau_1} = \frac{\Delta + s(1-\eta)}{\Delta + s(1+\eta)} \qquad \tau_2+\tau_1 = -(\Delta+s) \qquad \tau_2-\tau_1 = s\eta \qquad \tau_2\tau_1 = sm_{\tilde{e}}^2$$

the total cross-section is :

$$\boxed{\sigma = \frac{\pi\alpha^2}{s}\left[\eta(1+7\frac{\Delta}{s}) + 4\frac{\Delta}{s}(1+\frac{\Delta}{s})\ln\frac{\Delta+s(1-\eta)}{\Delta+s(1+\eta)}\right]}$$

If $m_{\tilde{\gamma}}^2 = 0$ this expression becomes :

$$\sigma_{\tilde{\gamma}\tilde{e}} = \frac{\pi\alpha^2}{s}\left[(1-\frac{m_{\tilde{e}}^2}{s})(1+7\frac{m_{\tilde{e}}^2}{s}) + 4\frac{m_{\tilde{e}}^2}{s}(1+\frac{m_{\tilde{e}}^2}{s})\ln\frac{m_{\tilde{e}}^2}{s}\right]$$

we can integrate it over the quasi-real photon spectrum in order to obtain the $\tilde{e}\tilde{\gamma}e$ production cross-section in e^+e^- collisions :

$$\sigma_{\tilde{e}\tilde{\gamma}e} = \int_\mu^1 dx f_\gamma(x)\sigma_{\tilde{e}\tilde{\gamma}}(xs) \qquad \text{con} \qquad f_\gamma(x) = \frac{\alpha}{2\pi}(\log\frac{s}{4m_e^2})(\frac{2}{x}-2+x)$$

Where $\mu = m_{\tilde{e}}^2/s$. We have after including both charged states :

$$\sigma_{\tilde{e}\tilde{\gamma}e} = \frac{\alpha^3}{m_{\tilde{e}}^2}\log\frac{s}{4m_e^2}\int_\mu^1(\frac{2}{x}-2+x)\frac{\mu}{x}[1+6\frac{\mu}{x}-7\frac{\mu^2}{x^2}+4\frac{\mu}{x}(1+\frac{\mu}{x})\ln\frac{\mu}{x}]$$

$$= \frac{\alpha^3}{s}\log\frac{s}{4m_e^2}\int_\mu^1 dx\left\{1 + (6\mu-2)\frac{1}{x} + (2-12\mu-7\mu^2)\frac{1}{x^2} + (12\mu+14\mu^2)\frac{1}{x^3} - 14\frac{\mu^2}{x^4}\right.$$
$$\left. + \left[8\frac{\mu^2}{x^4} + (8\mu-8\mu^2)\frac{1}{x^3} + (4\mu^2-8\mu)\frac{1}{x^2} + 4\frac{\mu}{x}\right]\ln\frac{\mu}{x}\right\}$$

$$= \frac{\alpha^3}{s}\log\frac{s}{4m_e^2}[-2\mu\ln^2\frac{1}{\mu} - 2(1-\mu-\frac{4}{3}\mu^2)\ln\frac{1}{\mu} + \frac{2}{9}(\frac{2}{\mu}+18-54\mu+34\mu^2)]$$

$$= \frac{\alpha}{6\pi}\sigma_{pt}\log\frac{s}{4m_e^2}[\frac{2}{\mu}+18-54\mu+34\mu^2 + 3(3-3\mu-4\mu^2)\ln\mu - 9\mu\ln^2\mu]$$

24

$\gamma\gamma \to \tilde{e}\tilde{e}$

The three Feynman diagrams relevant for this process are shown in figure A4; the total amplitude is :

$$T = -ie^2 \epsilon_\mu \epsilon'_\nu \left[\frac{(2q-k)^\mu (2q'-k')^\nu}{2qk} + \frac{(2q'-k)^\mu (2q-k')^\nu}{2qk'} - 2g^{\mu\nu} \right]$$

T can be written : $T = -ie^2 \epsilon_\mu \epsilon'_\nu T^{\mu\nu}$ with $k_\mu T^{\mu\nu} = k'_\nu T^{\mu\nu} = 0$ allowing the use of $\sum_{pol} \epsilon_\mu \epsilon_\nu = \sum_{pol} \epsilon'_\mu \epsilon'_\nu = -g_{\mu\nu}$. The squared and averaged amplitude is :

$$\begin{aligned}
\overline{|T|^2} =& \frac{e^4}{4} \Bigg[\frac{(2q-k)^2(2q'-k')^2}{(2qk)^2} + \frac{(2q'-k)^2(2q-k')^2}{(2qk')^2} + 16 \\
& - 4\frac{(2q-k)(2q'-k')}{2qk} - 4\frac{(2q'-k)(2q-k')}{2q'k} + 2\frac{(2q-k).(2q'-k)(2q'-k').(2q-k')}{(2qk)(2qk')} \Bigg] \\
=& \frac{e^4}{4} \Bigg[16 + \frac{(2q-k)^2(2q'-k')^2}{(2qk)^2} - 4\frac{(2q-k)(2q'-k')}{2qk} \\
& + \frac{2/s}{2qk}(2q-k).(2q'-k)(2q'-k').(2q-k') + (k \leftrightarrow k') \Bigg]
\end{aligned}$$

Using the relations :

$$\frac{(2q-k)^2}{2qk} = \frac{(2q'-k')^2}{2qk} = 2\left(\frac{m_{\tilde{e}}^2}{qk} - 1 \right)$$

$$(2q-k)(2q'-k') = 4qq' - 4kq' + kk'$$

$$(2q-k)(2q'-k) = (2q'-k')(2q-k') = 4qq' - s$$

We find :

$$\begin{aligned}
\overline{|T|^2} =& \frac{e^4}{4} \Bigg[16 + 4\left(\frac{m_{\tilde{e}}^2}{qk} - 1 \right)^2 - 2\frac{(4qq' - 4kq' + kk')}{qk} + \frac{1}{sqk}(4qq' - s)^2 + (k \leftrightarrow k') \Bigg] \\
=& \frac{e^4}{4} \Bigg\{ 16 + \left[16\frac{m_{\tilde{e}}^4}{(2qk)^2} - 16\frac{qq'}{2qk} + 16\frac{2(qq')^2}{2sqk} - 4 \right] + (k \leftrightarrow k') \Bigg\} \\
=& 4e^4 \Bigg\{ \frac{1}{2} + \frac{m_{\tilde{e}}^4}{(t - m_{\tilde{e}}^2)^2} + \frac{qq'}{t - m_{\tilde{e}}^2} - \frac{2(qq')^2}{s}\frac{1}{t - m_{\tilde{e}}^2} + (t \leftrightarrow u) \Bigg\} \\
=& 4.16\pi^2\alpha^2 \Bigg[\frac{1}{2} + \frac{m_{\tilde{e}}^4}{(t - m_{\tilde{e}}^2)} + \frac{m_{\tilde{e}}^2}{t - m_{\tilde{e}}^2}\left(1 - 2\frac{m_{\tilde{e}}^2}{s} \right) + (t \leftrightarrow u) \Bigg]
\end{aligned}$$

The angular distribution is :

$$\frac{d\sigma}{dt} = \frac{1}{16\pi s^2}\overline{|T|^2} = \frac{4\pi\alpha^2}{s^2}\left[\frac{1}{2} + \frac{m_{\tilde{e}}^4}{(t - m_{\tilde{e}}^2)^2} + \frac{m_{\tilde{e}}^2}{t - m_{\tilde{e}}^2}\left(1 - 2\frac{m_{\tilde{e}}^2}{s} \right) + (t \leftrightarrow u) \right]$$

which can also be written :

$$\boxed{\frac{d\sigma}{dt} = \frac{4\pi\alpha^2}{s^2}\left[1 - \frac{2m_{\tilde{e}}^2 s(ut - m_{\tilde{e}}^4)}{(t - m_{\tilde{e}}^2)^2(u - m_{\tilde{e}}^2)^2} \right]}$$

where $\tilde{e}_R$ and $\tilde{e}_L$ contributions have been included. In terms of $y = \cos\theta$, where θ is the center-of-mass frame scattering angle , we find :

$$\frac{d\sigma}{dy} = \frac{2\pi\alpha^2}{s}\beta_{\tilde{e}}\left[1 - \frac{2\beta_{\tilde{e}}^2(1 - \beta_{\tilde{e}}^2)(1 - y^2)}{(1 - \beta_{\tilde{e}}^2 y^2)^2} \right]$$

where we used :

$$t = m_{\tilde{e}}^2 - \frac{s}{2}(1 - \beta_{\tilde{e}}y) \qquad u = m_{\tilde{e}}^2 - \frac{s}{2}(1 + \beta_{\tilde{e}}y)$$

In order to compute the total cross-section, we define : $\tau = t - m_{\tilde{e}}^2$

$$\frac{d\sigma}{d\tau} = \frac{4\pi\alpha^2}{s^2}\left[\frac{1}{2} + \frac{m_{\tilde{e}}^4}{\tau^2} + \frac{m_{\tilde{e}}^2}{\tau}\left(1 - 2\frac{m_{\tilde{e}}^2}{s} \right) + (t \leftrightarrow u) \right]$$

25

u and t terms give equal contributions so :

$$\sigma = \frac{4\pi\alpha^2}{s^2} \int_{\tau_1}^{\tau_2} d\tau \left[\frac{1}{2} + \frac{2m_{\tilde{e}}^4}{\tau^2} + \frac{2m_{\tilde{e}}^2}{\tau} \left(1 - 2\frac{m_{\tilde{e}}^2}{s} \right) \right]$$

$$= \frac{4\pi\alpha^2}{s^2} \left[(\tau_2 - \tau_1) \left(\frac{1}{2} + \frac{2m_{\tilde{e}}^4}{\tau_1 \tau_2} \right) + 2m_{\tilde{e}}^2 \left(1 - 2\frac{m_{\tilde{e}}^2}{s} \right) \ln \frac{\tau_2}{\tau_1} \right]$$

with :

$$\tau_1 = -\frac{s}{2}(1 + \beta_{\tilde{e}}) \qquad \tau_2 = -\frac{s}{2}(1 - \beta_{\tilde{e}})$$

then :

$$\tau_2 - \tau_1 = s\beta_{\tilde{e}} \qquad \tau_1 \tau_2 = s m_{\tilde{e}}^2$$

and finally :

$$\sigma = \frac{4\pi\alpha^2}{s} \beta_{\tilde{e}} \left[\frac{1}{2} + 2\frac{m_{\tilde{e}}^2}{s} - \frac{2m_{\tilde{e}}^2}{s\beta_{\tilde{e}}} \left(1 - 2\frac{m_{\tilde{e}}^2}{s} \right) \ln \frac{1 + \beta_{\tilde{e}}}{1 - \beta_{\tilde{e}}} \right]$$

or :

$$\boxed{\sigma = \frac{4\pi\alpha^2}{s} \beta_{\tilde{e}} \left[2 - \beta_{\tilde{e}}^2 - \left(\frac{1 - \beta_{\tilde{e}}^4}{2\beta_{\tilde{e}}} \right) \ln \frac{1 + \beta_{\tilde{e}}}{1 - \beta_{\tilde{e}}} \right]}$$

After including $\tilde{e}_R$ and $\tilde{e}_L$ contributions.

The relevant formula for $e^+ e^-$ interactions is of course :

$$\sigma_{\tilde{e}\tilde{e}ee} = \int\int dx_1 dx_2 f_\gamma(x_1) f_\gamma(x_2) \sigma_{\gamma\gamma \to \tilde{e}\tilde{e}}(x_1 x_2 s)$$

Where the integration region is $x_1 x_2 s < 4m_{\tilde{e}}^2$ and $f_\gamma(x)$ has been defined previously. The equivalent photon approximation has been again used.
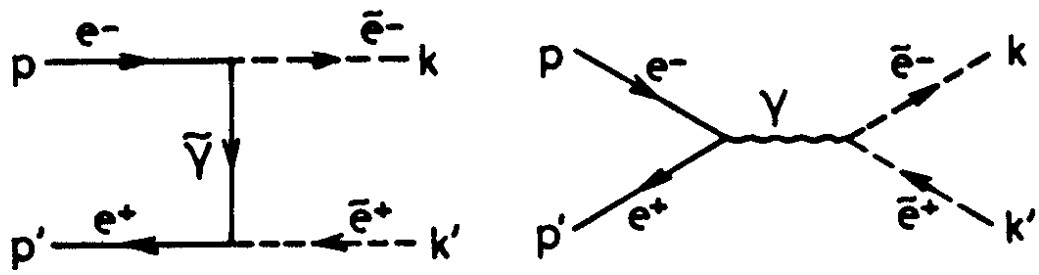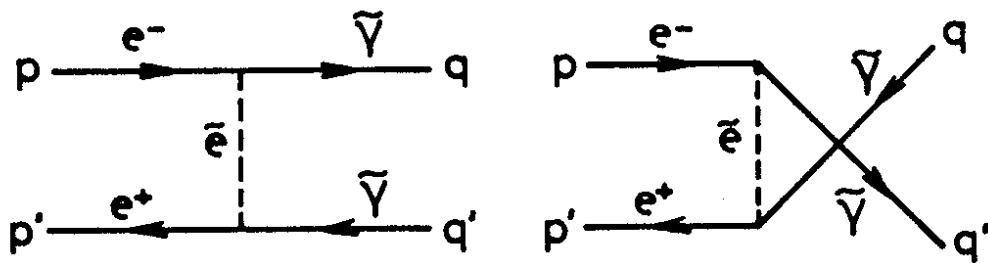
Fig. A1

Fig. A2

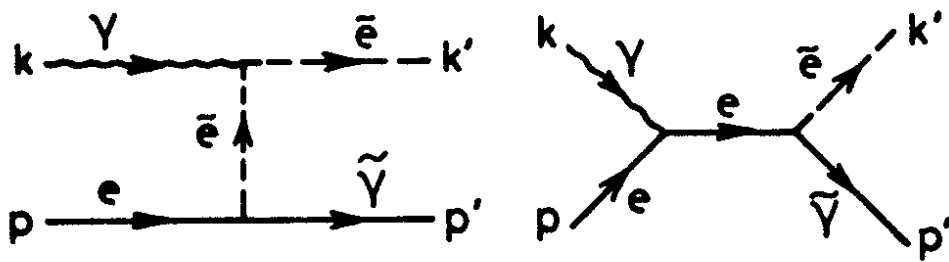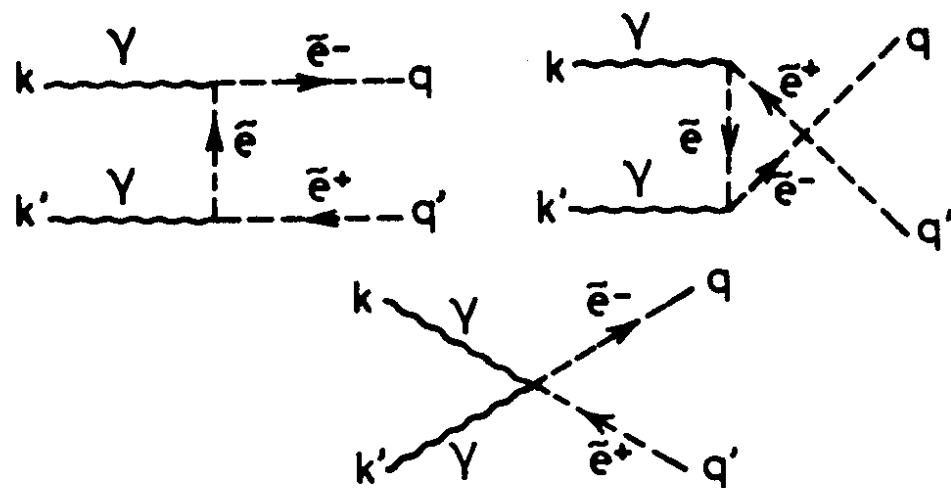Fig. A3

Fig. A4

7-REFERENCES

[1]   P.Fayet,S.Ferrara, Phys.Rep.$C32$(1977)249

[2]   G.Farrar,P.Fayet, Phys.Lett.$89B$(1980)191

[3]   M.Glück,E.Reya, Phys.Lett.$130B$(1983)423

[4]   P.Fayet, Phys.Lett.$117B$(1982)460

[5]   J.Ellis,J.Hagelin, Phys.Lett.$122B$(1983)303

[6]   M.K.Gaillard,L.Hall,I.Hinchliffe, Phys.Lett.$116B$(1982)279

[7]   M.Glück, Phys.Lett.$129B$(1983)255

       T.Kobayashi,M.Kuroda, Phys.Lett.$134B$(1984)271

       J.Grifols,R.Pascual, Phys.Lett.$135B$(1984)319

[8]   T.Kobayashi,M.Kuroda, Phys.Lett.$139B$(1984)208

       J.Ware,M.Machacek, Phys.Lett.$142B$(1984)300

       K.Grassie,P.Pandita, Phys.Rev.$D30$(1984)22

[9]   N.Cabibbo,G.Farrar,L.Maiani, Phys.Lett.$105B$(1981)155

[10]   K.J.F.Gaemers,R.Gastmans,F.M.Renard, Phys.Rev.$D19$(1979)1605

[11]   CELLO preliminary results

[12]   JADE Coll., Phys.Lett.$139B$(1984)325

[13]   JADE Coll., Phys.Lett.$152B$(1985)385

[14]   TASSO Coll., Z.Phys.$C26$(1984)337

[15]   MARK J Coll., MIT Technical Report 139(1984)

[16]   MARK J Coll., MIT Technical Report 141(1984)

[17]   MARK II Coll., Phys.Rev.Lett.51(1983)2253

[18]   MAC Coll., Phys.Rev.Lett.52(1984)22

[19]   MAC Coll., Phys.Rev.Lett.54(1985)1118

[20]   R.Hollebeek, SLAC-PUB-3347(1984)

[21]   C.Weizsäcker,E.T.Williams, Z.Phys.88(1934)612

[22]   G.Bonneau,F.Martin, Nucl.Phys.$B27$(1971)381

[23]   CELLO Coll., Phys.Lett.$114B$(1982)287

[24]   TASSO Coll., Phys.Lett.$117B$(1982)365

[23]   CELLO Coll., Phys.Lett.$122B$(1983)127